Society for Pediatric Pathologists

Abstracts of the 2022 Spring Meeting

March 19 – 20, 2022

Virtual Meeting

PLATFORM I: Pediatric/Genomics

1

Incidence of Multiple Fusion Genes in Pediatric Malignancy: Application of a Novel Fusion Classification System to Determine Clinical Significance

A MacKeracher, R Siddaway, A Arnoldo, G Somers; Hospital for Sick Children, Toronto, Ontario

Background: The implementation of next-generation sequencing in combination with sensitive software tools for cancer diagnosis has markedly increased the ability to detect genetic abnormalities. Such assays have resulted in accurate diagnoses and allowed precision medicine to evolve. Consequently, sequence nucleotide variants (SNVs) and fusion genes are being discovered at an exponential rate. As of 2017, several organizations (e.g., the Association of Molecular Pathology; the College of American Pathologists) have established a standardized classification model for SNVs using a 4-tier classification system, stratifying SNVs into distinct clinical categories. However, no such classification system has been developed for novel fusion genes. In addition, examples of tumours harboring more than one fusion gene are being increasingly discovered. This study aims to determine the number of tumour samples with more than one fusion and utilizes a novel fusion gene classification system to classify fusion genes.

Methods: Fifty-three bone and soft tissue tumours and external QA samples underwent RNA extraction and sequencing using the Illumina TruSight pan-cancer assay modified for pediatric use. The results were analyzed by the Metafusion (MF) software package. The number of tumours with a single fusion gene and those with more than one fusion gene were calculated. All fusions were then classified into three categories using a modification of the SNV classification system as follows: tier 1 (strong clinical significance) were fusions where both genes have been reported together in large studies in the same cancer and where functional studies confirmed pathogenicity. Fusions were classified as tier 2 (potential clinical significance) if at least one of the fusion genes was seen to be tier 1 pathogenic; or if the fusion was reported in other tumour types; or if the fusion was reported in small studies without functional data. Fusions were classified as tier 3 (unknown clinical significance) if none of the above criteria were met.

Results: The sequencing data for the 53 samples were analyzed using the MF software, and 106 fusion genes were detected. From these samples, 29 had a single fusion and 24 had more than one fusion. However, no samples with more than one fusion had more than one tier 1 fusion. Overall, there were 18 tier 1 fusions, 30 tier 2 fusions and 58 tier 3 fusions.

Conclusion: Forty-five percent of samples analyzed had more than one fusion gene. None had more than one tier 1 fusion gene. Overall we show the utility of a novel classifier in determining potential pathogenicity and clinical relevance of fusion genes, and hope that this study will contribute to the future establishment of clear guidelines for the classification of fusion transcripts.

2

Genome-wide Identification of Potential Methylation-regulated Genes and Pathways in Hepatocellular Malignant Neoplasm, NOS

S Zhou[1], M Li[2], D Ostrow[1], D Ruble[1], L Mascarenhas[1], B Pawel[1], T Triche[1]; [1]Children's Hospital Los Angeles, Los Angeles, California; [2]USC Libraries Bioinformatics Services, Los Angeles, California

Background: Hepatocellular malignant neoplasm, not otherwise specified (HCN-NOS), is a provisional diagnostic entity with histology features of neither typical hepatoblastoma (HB) nor hepatocellular carcinoma (HCC). The molecular basis of HCN-NOS is unknown. We aimed to obtain insights into gene expression changes and to identify potential methylation-regulated genes and pathways.

Methods: Parallel genome-wide profiling of gene expression and DNA methylation was performed on 4 pairs of pre-treatment HCN-NOS tumors and adjacent non-tumor tissue controls. RNAseq and DNA methylation profiling data were first analyzed using Partek Flow and Partek® Genomics Suite® software, respectively, and then further analyzed by the Ingenuity Pathway Analysis (IPA). Gene expression of some aberrantly methylated-differentially expressed genes in HCN-NOS were validated using an independent set of HCC data archived in TCGA TARGET. The protein expression of 4 up-regulated genes by RNAseq were validated by immunohistochemical staining.

Results: There were 2530 significantly differentially expressed genes (DEGs) between tumors and controls. Many DEGs were associated with HB and or HCC. Pathways in the categories of "Cellular Growth" and "Cell Cycle Regulation" were predominantly enriched. Analysis Match in IPA found that the gene expression profiling of HCN-NOS was unique but significantly similar to that of both HB and HCC. A total of 27,195 CpG sites (CpGs) were significantly differentially methylated (DM) between tumors and controls with a global hypomethylation pattern concomitant with predominant CpG island (CGI) hypermethylation in promotor regions. Developmental process and molecular function regulators were predominantly affected by aberrant DNA methylation. The most enriched canonical pathway of DM CGIs was Transcriptional Regulatory Network in Embryonic Stem Cells. A total of 1055 aberrantly methylated (at CpGs) and expressed genes were identified, including 25 upstream regulators and sixty-one potential CpG island methylation-regulated genes. Furthermore, nine of the 61 genes (HAND2, CES4A, SORBS1, GADD45B, SP6, SRC, MAZ, TCF3 and C14orf180) showed consistent expression patterns in public HCC datasets. Additionally, 8 potential DNA methylation-regulated genes (TCF3, MYBL2, SRC, HMGA2, COL2A1, MYCN, PPARGC1A and SLC22A1) found in HCN-NOS demonstrated prognostic values in HCC patients. The protein expression results of glypican 3, SALL4, HMGA2 and FOXM1 in HCN-NOS were consistent with the gene expression data obtained by RNAseq.

Conclusion: HCN-NOS had a unique gene expression and DNA methylation profile. Many potential DNA methylation-regulated genes associated with HCC were identified.

3

Infantile Hemispheric Glioma and Desmoplastic Infantile Ganglioglioma/ Astrocytoma Show Genomic and Epigenomic Overlap and Have Near Universal Long-Term Survival

A Gilani[1], Z Siddiq[2], B Kleinschmidt-DeMasters[2]; [1]Childrens Hospital Colorado, University of Colorado, Aurora, Colorado; [2]University of Colorado, Aurora, Colorado

Background: Gliomas are broadly divided into pediatric-type and adult-type based on molecular features. Infant-type hemispheric glioma (IHG) (AKA congenital glioblastoma /cGBM) is a particularly interesting subtype within pediatric-type gliomas that frequently harbor ALK, ROS1, NTRK or MET gene fusions and typically has a better outcome than other high-grade gliomas. Another tumor entity presenting in the infantile age group is the desmoplastic infantile ganglioglioma / astrocytoma (DIA), which is characterized clinically by large solid/ cystic supratentorial tumors, and histologically by astrocytic and ganglionic components, extensive reticulin-rich desmoplastic stroma and fibroblast-like spindle-shaped cells. Although described as a grade 1 tumor, DIA often has primitive, embryonal-like foci, which can show increased proliferative activity as well as necrosis, making the distinction from IHG difficult. In order to understand the similarities and differences between IHG and DIA, we studied their histologic, molecular, and clinical characteristics.

Methods: 7 patients with IHG and 6 with DIA were identified (histologic findings previously reported in PMIDs: 31875306, 27860162). All tumors were supratentorial and presented in 1st yr of life. Genomic testing was performed using 500+ gene (or 50 genes in a subset) NGS-based DNA and RNA panels. DNA methylation testing was performed on Illumina EPIC 850K array. T-distributed stochastic neighbor embedding (t-SNE) and differentially methylated region (DMR) analysis were performed using bioconductor based packages on R. For classification, Idat files were uploaded to the DKFZ/Heidelberg CNS tumor classifier (version 12.3) website.

Results: 3/6 cases of IHG that underwent targeted NGS fusion mutation panel were positive for fusions involving the ALK gene, and 1/6 showed GOPC:ROS1 fusion. Interestingly, 1/5 cases with histologic diagnosis of DIA also featured GOPC:ROS1 fusion. 1/5 DIA cases showed BRAF V600D mutation. DNA methylation profiling identified 2/5 DIA cases as IHG (including the one with ROS1 alteration), 1/5 as DIA, and the remaining 2/5 as ganglioglioma or teratoma. tSNE showed clustering of all 5 histologically defined DIA cases with or near IHG reference cases. IHG cases were also epigenomically heterogenous with 2/3 cases that underwent methylation analysis classified as methylation class-IHG and 1/3 as no match on the Heidelberg classifier. Despite the heterogenous genomic and epigenomic profiles, all 6 DIA and 6/7 IHG cases showed long term survival and remain free of tumor recurrence.

Conclusion: These data highlight the genomic and epigenetic overlap between histologically defined DIA and IHG cases and suggest that appropriate surgical resection can lead to long-term survival in both entities.

4

Morphologic Features in Congenital Pulmonary Airway Malformations and Pulmonary Sequestrations Correlate with KRAS Mutation Status

N Nelson[1], F Xu[2], M Li[2], J Pogoriler[2]; [1]University of Pennsylvania, Philadelphia, Pennsylvania; [2]Children's Hospital of Philadelphia, Philadelphia, Pennsylvania

Background: We previously presented data showing most type 1 and 3 congenital pulmonary airway malformations (CPAMs) harbor an activating KRAS mutation, suggesting they arise secondary to these mutations. By contrast, the etiology of type 2 CPAMs is unknown. Previously published data suggest many CPAMs are due to bronchial atresia during development, and type 2 CPAMs morphologically resemble the cystic maldevelopment sometimes seen in intra- and extra-lobar sequestrations (ILS and ELS), which lack normal airway connections. We hypothesized that type 2 CPAMs, ILS, and ELS would be negative for KRAS mutations, consistent with an origin secondary to obstructive physiology and distinguishing them from type 1/3 CPAMs. Because mutation status is not routinely assessed clinically, cyst size is not a perfect surrogate, and some historic diagnostic criteria are difficult to apply, we sought to determine histologic features that correlate with mutation status in order to improve classification and guide management.

Methods: Morphologic features were evaluated by two pathologists. Regions of interest were enriched via macrodissection of FFPE tissue, DNA was extracted, and exon 2 of KRAS was amplified using PCR. PCR products were Sanger sequenced and analyzed using Mutation Surveyor(SoftGenetics,PA).

Results: Approximately 80% of ILS and ELS had a large airway associated with the feeding vessel. Features that did not show significant correlation with overall classification included epithelial lining type, presence of alveoli intermixed between cysts and presence of cartilage.

	N	*KRAS* mutation	Median corrected gestational age (weeks)	Mucostasis	Largest cyst size (mean ± SD) cm	Complex epithelium	Mucinous cell clusters (MCC)	Simple round cysts	Frequent cyst/ alveolar transitions
Type 1/3	91	83 (91%)	38	4 (4%)	2.8±1.6	64 (70%)	66 (73%)	0 (0%)	76 (84%)
Type 2	23	0 (0%)	44	18 (78%)	1.1±0.5	1 (4%)	0 (0%)	18 (78%)	3 (13%)
ILS	11	0 (0%)	44	11 (100%)	0.7±0.4	1 (9%)	0 (0%)	3 (27%)	1 (9%)
ELS	10	0 (0%)	41	5 (50%)	0.58±0.4	3 (30%)	0 (0%)	6 (60%)	0 (0%)
P value		<0.0001	>0.05	<0.0001	<0.0001	<0.0001	<0.0001	<0.0001	<0.0001

Conclusion: Type 2 CPAMs and cystic ILS and ELS do not harbor KRAS exon 2 mutations. Cases lacking mutation are more likely to demonstrate features of obstruction and to have simple shaped cysts which are <2 cm and rarely directly communicate with alveolar-type spaces or show complex epithelial patterns. We hypothesize that this lack of complexity may be due to the absence of a mutation driving epithelial proliferation.

5

Distinct immunophenotypic features of novel genetic subtypes of pediatric B-lymphoblastic leukemia are recognizable in a clinical setting and can help direct molecular testing

M Takeda[1], M Wengyn[2], D Bhojwani[3], Z Gu[4], B Wood[5], G Raca[5], A Kovach[5]; [1]Pathology and Laboratory Medicine, Children's Hospital Los Angeles, Los Angeles, California; [2]Miller School of Medicine, University of Miami, Miami, Florida; [3]Hematology/Oncology, Children's Hospital Los Angeles, Los Angeles, California; [4]Computational and Quantitative Medicine & Systems Biology, City of Hope, Duarte, California; [5]Laboratory Medicine, Children's Hospital Los Angeles, Los Angeles, California

Background: B-lymphoblastic leukemia (B-ALL), the most common malignancy of childhood, is characterized by diverse cytogenomic (CG) drivers that dictate clinical behavior and prognosis. Subclassification is increasingly complex, costly and time intensive. Some immunophenotypic (IP) features are highly associated with subtype and can be available within hours, helping direct CG testing, e.g. lack of CD10 in KMT2A-rearranged (KMT2A-R) B-ALL and CRLF2 in ~50% of BCR-ABL1-like (Ph-like) B-ALL. IP features in some novel genetic subtypes, where CG features may be inapparent by current standard-of-care testing, also appear to be recurrent, e.g. variable/decreased CD10 in DUX4 and ZNF384-R B-ALL. Such IPs have been characterized in large adult (Paietta Blood 2021) and pediatric (Ohki Genes Chromosomes Cancer 2020) research cohorts. We hypothesized that IP review of novel B-ALL subtypes at our institution would confirm these features and inform future prospective CG work-up in clinical settings.

Methods: Retrospective clinical flow cytometric antigen expression data from 358 genetically characterized B-ALL at diagnosis or relapse were reviewed. Assessed antigens (CD2, CD5, CD7, CD9, CD10, CD13±CD33, CD14, CD19, CD20, CD22, CD24, CD34, CD45, CD64, CD123, CRLF2 and cMPO) were evaluated for intensity (increased, expected, decreased, absent) and distribution (uniform, variable, partial) compared to that expected for normal early B precursors (stage I hematogones). CG features were determined by clinical [karyotype, FISH, pediatric cancer DNA and RNA panel (OncoKids®), CMA] and/or research (RNAseq, optical genome mapping) assays.

Results: Our cohort included the following novel B-ALL subtypes: DUX4-R (5 cases, 1.4%), ZNF384--R [8, 2.2%, including 3 MPAL B/Myeloid], MEF2D--R (3, 0.8%), PAX5Alt (4, 1.1%) and PAX5 P80R (1, 0.2%). In DUX4-R, CD10 was variably decreased (4/5) or uniform at the expected intensity (1/5); CD2 was expressed in 1/4 assessed cases. In ZNF384--R, CD10 was absent (5/8) or variably decreased (3/8). In MEF2D--R, CD9 was uniformly increased (3/3), CD5 partially expressed (1/2 assessed cases) and CD10 inconsistent (expected, variable/decreased, uniform/increased). PAX5Alt showed heterogenous driver lesions [intragenic tandem multiplication (2) and PAX5::FOXP1 and PAX5::PML rearrangements (1 each)] and no notable IP features.

Conclusion: In our large pediatric B-ALL clinical cohort, novel genetic subtypes show IP features expected from research reports, some of which can inform CG evaluation given high specificity although lower sensitivity. Future directions include systematic IP characterization of all cohort cases; sensitivity, specificity, and positive/negative predictive value assessment of IP combinations by genetic subtype; and prospective evaluation of novel IP markers.

6

Papillary Hemangiomas Harbor GNA11 and GNAQ Mutations

C Gestrich[1], M Vivero[1], D Konczyk[1], J Goss[1], C Cottrell[2], G Pearson[3], M Mathew[2], V Prasad[3], H Kozakewich[1], C Fletcher[4], A Greene[1], A Al-ibraheemi[1]; [1]Boston Children's Hospital, Boston, Massachusetts; [2]Nationwide Children's Hospital, Institute for Genomic Medicine, Columbus, Ohio; [3]Nationwide Children's Hospital, Columbus, Ohio; [4]Brigham and Woman's Hospital, Boston, Massachusetts

Background: Papillary hemangioma (PH) is a small, primarily dermal lesion occurring predominantly in the head and neck region in children and adults. Its signature characteristics are dilated thin-walled channels containing papillations with capillarous vasculature and endothelial cytoplasmic eosinophilic inclusions. Molecular alterations in PH have not been reported.

Methods: Clinical, histopathologic, and genomic data was collected from two quaternary children's hospitals following clinically indicated procedures. Genomic DNA from one patient's lesion and blood was subject to paired whole exome sequencing (WES). DNA from formalin fixed paraffin embedded tissue from six additional PH lesions was extracted and Droplet digital PCR was utilized to confirm both the presence of and variant allele frequency for the loci found during WES and additional hot-spots.

Results: **T**he surgical and consultative files yielded seven PHs with FFPE tissue available for ddPCR. All presented in first four years, one being noted at birth. All, except one, were in the head and neck, were bluish, and ranged from 0.5 to 2.7 cm. (Table) Histologic examination showed dermal nodules, some with extension into subcutaneous fat. There were one or more dominant nodules delineated by a thin-walled vessel with papillary formation, and a variable number of endothelial cells with cytoplasmic eosinophilic inclusions. Some PH also had smaller capillarous nodules without papillations and few or no endothelial cytoplasmic inclusions. Small thrombi were seen in four PH. Five lesions had *GNA11* p.Q209L and 2 had *GNAQ* p.209L missense mutations.

Patient # Sex	Age at presentation	Age at excision (Y)	Location	Size (cm)	Mutation
1 M	Birth	8	Neck	2.5	GNA11 A6626T Q209L
2 F	14 months	3	Post auricular	≤ 1.8	GNA11 A6626T Q209L
3 M	2 years	3.5	Lip	0.6	GNA11 A6626T Q209L
4 F	Unknown	4	Post auricular	2.1	GNAQ A626T Q209L
5 F	3 years	4	Lip	0.5	GNA11 A6626T Q209L
6 M	3 years	7	Arm	1.2	GNA11 A6626T Q209L
7 F	4 years	12	Scalp	2.8	GNAQ A626T Q209L

Conclusion: PHs contain GNA11 and GNAQ p.Q209L mutations. These genes are closely related and are involved in MAPK and/or YAP signaling. Mutations in GNA11 and GNAQ are associated with other types of somatic vascular lesions: capillary malformation, congenital hemangioma, anastomosing hemangioma, thrombotic anastomosing hemangioma, and hepatic small cell neoplasm. This might account for some overlapping clinical and pathologic features in these entities, perhaps explicable by the timing of the mutation or influence of the germline phenotype.

7

Is karyotype still warranted? A two-year study comparing chromosome and whole-genome array analyses in pediatric solid tumors

B Kang, H Xiao, A Heider, C Simon, R Rabah, L Shao; University of Michigan Medical School Department of Pathology, Ann Arbor, Michigan

Background: Conventional cytogenetics has played a pivotal role in the detection of recurrent chromosomal abnormalities in pediatric tumors. Cytogenetic and complementary microarray analysis on tumor cells are becoming increasingly essential for the diagnosis of pediatric tumors, prediction of the patients' prognosis, and placement on appropriate targeted therapies. Pathologists are increasingly provided smaller needle biopsies for upfront diagnosis and appropriate triage of precious tumor specimens is extremely important. Cytogenetic analysis of small samples might be compromised due to lack of mitosis in tumor cells or overgrowth by normal cells. Whole-genome array analysis provides increased genomic resolution and more accurate analysis of the underlying genetic profile over classical cytogenetics even with a small amount of DNA. We compared the yield of conventional karyotype and whole-genome array analysis for the workup of pediatric tumors at our institution.

Methods: We retrospectively reviewed results of conventional cytogenetics and whole-genome array results for all pediatric tumor samples submitted fresh to the cytogenetic laboratory at our institution from Dec 2019 -Nov 2021. The whole-genome array analysis was performed using the Thermo Fisher CytoScan platform.

Results: A total of 195 samples were tested by both karyotype and whole-genome array analysis. Out of 195 samples, 125 samples (64.1%) had at least one copy number aberrations or region of loss of heterozygosity detected by the whole-genome array. 30 out of 125 (24%, 15.4% of the total samples) had an abnormal karyotype, and the remaining 95 samples had a normal karyotype (35.2%) or inadequate cells for cytogenetic analysis (40.8%). Seventy samples (35.9%) showed a normal array result, 38 of them (54.3%) had a normal karyotype and 32 (45.7%) had inadequate cells for cytogenetic analysis. There were no discordant results between normal array results and karyotype results. Five cases with abnormal karyotype showed balanced inversion (1) or translocation (4) which were not detected by the whole-genome array. Among them, a t(16;21)(p11.2;q22) in one patient with metastatic Ewing sarcoma was clinically significant. This translocation was previously detected at diagnosis from a bone biopsy. The abnormalities in the other cases were not associated with any known diagnostic or prognostic significance.

Conclusion: Based on our experience, the array studies demonstrated a greater number of genomic alterations than the standard cytogenetic analyses. We suggest that array analysis should be prioritized over conventional cytogenetics in daily practice when faced with limited samples from pediatric tumors.

8

Validation of a Nationwide Digital Pediatric Pathology Consultation Service

H Chen[1], J Putra[1], A Nagy[1], J Terry[2], D El Demellawy[3], J de Nanassy[3], E Schollenberg[4], A Haig[5], C Stefanovici[6], K Whelan[7], A Poulin[8], D Dal Soglio[9], Z Chen[9], G Somers[1]; [1]The Hospital for Sick Children, Toronto; [2]BC Children's Hospital, Vancouver, British Columbia; [3]Children's Hospital of Eastern Ontario, Ottawa, Ontario; [4]IWK Health Centre, Halifax, Nova Scotia; [5]London Health Sciences Centre, London, Ontario; [6]University of Manitoba, Winnipeg, Manitoba; [7]Janeway Children's Health & Rehabilitation Centre, St John's, Newfoundland and Labrador; [8]Saskatchewan Health Authority, Saskatoon, Saskatchewan; [9]CHU Sainte-Justine, Montreal, Quebec

Background: Seeking second opinion consultations is an important tool when faced with difficult, rare and challenging biopsy material. This is especially so in pediatric pathology, where rare and uncommon conditions are diagnosed on a daily basis. However, packaging and sending glass slides and paperwork is time-consuming, costly and can result in delays in diagnosis. To this end, pediatric pathologists in nine hospitals across Canada formed a digital pathology network to facilitate a timely second-opinion pathology service. This study outlines our unique validation process of forming such a nationwide pediatric pathology consultation service.

Methods: The study included one initiating hospital and eight partner hospitals. A total of 60 pathology cases were used, predominantly comprising pediatric malignancy. In part one of the study, 30 cases were selected by the initiating hospital. One H&E slide and one to two immunostain slides (if applicable) from each case were scanned to produce digital whole slide images (WSI). Glass slides were then sent from the initiating hospital to the eight partner hospitals for diagnostic interpretation. After a washout period of at least two weeks, the WSI were uploaded to a secure website and were interpreted by the same pathologists in the eight partner hospitals. Intra-observer diagnostic concordance (glass slide vs. digital image) was calculated. In part two of the study, the participating hospitals contributed a total of 30 cases to the initiating hospital. The cases went through a similar process of conversion to WSI, and both glass slides and WSI were reviewed at the initiating hospital with an appropriate washout period between the reviews. Intra-observer diagnostic concordance (glass slide versus digital image) was calculated. Concordance grading was performed in the initiating hospital by three pediatric pathologists, and a rate of >95% concordance for successful validation was used as per College of American Pathologists (CAP) guidelines.

Results: The study generated 269 diagnostic data points and 149 immunostain interpretation data points for concordance grading. Out of the 269 diagnostic data points, 257 were concordant (95.5%). All immunostain data points were concordant (100%). Combining the diagnostic and immunostain data together, the overall concordance rate was 97.1%.

Conclusion: This is a unique nationwide validation study for a large digital pediatric pathology network. The study included many pathologists and pathology cases from nine hospitals across Canada. A diagnostic concordance rate of 95.5% was achieved between glass slides and digital images, confirming that the nationwide digital pathology platform is a reliable method for second-opinion pathology consultations.

9

Intraoperative consultation in pediatric bone and soft tissue lesions: analysis of discordance and diagnostic pitfalls

B Coiner[1], J Liang[2], H Correa[2], J Johnson[2], H Wang[2]; [1]Vanderbilt University School of Medicine, Nashville, Tennessee; [2]Vanderbilt University Medical Center, Nashville, Tennessee

Background: Frozen section (FS) analysis is a well-established method of intraoperative consultation used to guide immediate surgical management in both adult and pediatric surgical pathology. Correlation of intraoperative impression with final diagnosis is an important aspect of quality assurance. However, little information is available on FS-permanent discordance in pediatric pathology, especially in pediatric bone and soft tissue (BST) lesions.

Methods: All pediatric surgical pathology cases from 2015 through 2020 at the study institution were queried for BST lesions and use of intraoperative consultation. Case details, intraoperative impression, and corresponding final diagnosis were retrospectively assessed for concordance.

Results: A total of 299 cases of pediatric BST lesions (188 bone and 111 soft issue) with intraoperative consultation and final histologic diagnosis were identified. Discordance between FS and final diagnosis was found in 25 cases (8.4%). Pathologist interpretation and sampling errors contributed to discordance in 76.0% (n=19) and 27% (n=7) of cases, respectively. The discordance rates for bone, soft tissue, benign, and malignant lesions were 6.4%, 11.7%, 8%, 9%, respectively. For tumor site, head and neck soft tissue lesions had the highest discrepancy rate of 19.4% (6/31). Specimens with higher complexity or multiple parts had greater rates of discordance (18.2% and 11.3%, respectively) compared to simple or single-part cases (7.6% and 7.1%, respectively). For FS purposes, the discordance rates for intraoperative triage, margin status, and tissue adequacy were 7.4%, 10.1%, and 40%, respectively. Nasopharyngeal angiofibromas (3/6, 50%), benign bone cysts (3/47, 6.4%), and Ewing sarcomas (3/22, 13.6%) had the highest incidence of discordance. However, only the association of nasopharyngeal angiofibroma with discordance was statistically significant ($p < 0.01$). In the 3 discordant cases of nasopharyngeal angiofibroma, indistinct tumor border and bland morphology of neoplastic spindle cells overlapping with reactive fibroblasts contributed to gross sampling and microscopic interpretation errors, respectively.

Conclusion: Intraoperative evaluation is a valuable tool for guiding surgical management of pediatric BST lesions with a low discordance rate. Soft tissue lesions of the head and neck, particularly nasopharyngeal angiofibromas, are challenging entities and represent significant diagnostic pitfalls.

PLATFORM II: GI/Cardiac

10

Online Atlas of High-Resolution 3D Reconstructions of Congenital Heart Defects Generated by Microfocus Computed Tomography

T Yamasaki[1], S Toba[1], K Mori[2], K Umezu[3], S Sanders[4], K Carreon[4]; [1]Boston Children's Hospital & Mie University Graduate School of Medicine, Boston, Massachusetts; [2]Mie University Faculty of Medicine, Tsu, Japan; [3]Mie University Graduate School of Medicine, Tsu, Japan; [4]Boston Children's Hospital & Harvard Medical School, Boston, Massachusetts

Background: Because of its complexity, understanding the anatomy of congenital heart defects (CHD) using two-dimensional resources can be challenging. Three-dimensional (3D) models of CHD can be produced using clinical computed tomography (CT). However, CT resolution is limited and it is impossible to reproduce thin and delicate structures such as valve leaflets and chordae. In this study, we scanned archived human postmortem wax-infiltrated heart specimens with CHD using microfocus-CT (micro-CT) to create a high-resolution 3D interactive atlas of CHD.

Methods: Human postmortem wax-infiltrated heart specimens from The Cardiac Registry of our institution were scanned using micro-CT (X-Tek HMXST225, Nikon Metrology, Inc.), and reconstructed to create 3D models using ImageJ (available at https://imagej.nih.gov/ij/) and Slicer (available at https://download.slicer.org/). The models were down-sampled using Meshlab (available at https://www.meshlab.net/) and published online on Sketchfab as a 3D atlas.

Results: The 57 specimens included in this study were obtained during 1973-2002 from deceased patients ages 1 day-52 years. The collection includes models of normal heart, atrial septal defect, ventricular septal defect, complete atrioventricular canal defect, tetralogy of Fallot, transposition of the great arteries, double outlet right ventricle, arch anomalies, hypoplastic left heart syndrome, heterotaxy syndrome, and others. Nine specimens had undergone palliative surgeries. The resolution of micro-CT was 25-119 micrometers (isotropic voxel size). The 3D models were uploaded on Sketchfab and anatomical structures were labeled on the models (Figure). The view may be freely manipulated and magnified to display intricate internal structures. Relevant clinical history and complete anatomic findings were also provided for each model. Additionally, high-quality models have been successfully printed using high-resolution 3D-printers. Figure: Original wax-infiltrated heart specimen of hypoplastic left heart syndrome is shown along with its representative micro-CT images. The high-resolution 3D printed resin model and digital model from the online atlas generated from the reconstructed micro-CT images are also shown. Note the excellent resolution of fine structures such as valve leaflets and chordae (arrows) in the two bottom photos as viewed from the apex. Note the labeling on the atlas model.

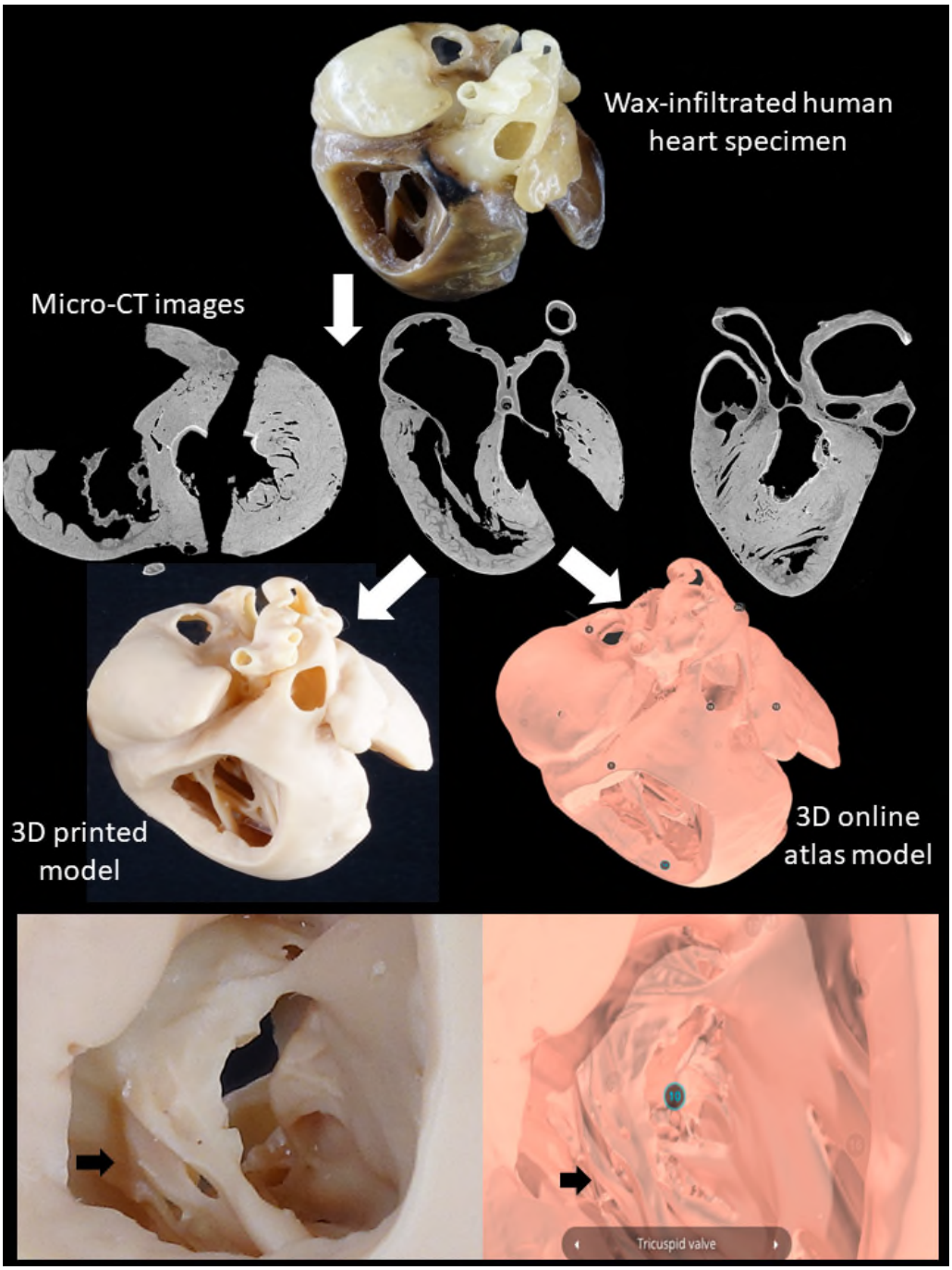

Conclusion: In conclusion, wax-infiltrated heart specimens are suitable for creating a digital high-resolution 3D interactive atlas of CHD. The digital atlas is now available at https://www.sketchfab.com/heartmodels/collections. We believe it will facilitate understanding complex CHD.

11

Morphologic and Morphometric Characterization of Juvenile Polyps with Genetic Correlation in Juvenile Polyposis

C Sande[1], G Brodeur[2], M Dent[2], M Duvall[2], B Greed[2], S Macfarland[2], B Wilkins[2]; [1]Hospital of the University of Pennsylvania, Philadelphia, Pennsylvania; [2]Children's Hospital of Philadelphia, Philadelphia, Pennsylvania

Background: Juvenile polyposis syndrome (JPS, OMIM 174900) is an autosomal dominant polyposis and cancer predisposition syndrome. A subset of patients have a germline pathogenic variant in SMAD4 or BMPR1A. A single prior study (PMID 21412070) has correlated colonic polyp morphology with genotype: lobulated, epithelial-predominant (stroma-poor) juvenile polyps (JP) accounted for a majority of SMAD4-associated polyps and a minority of BMPR1A-associated polyps, but were nearly absent in patients without germline mutation. The goals of this project were to characterize the histologic variety of polyps in a genetically-defined JPS cohort, test the observation that polyp morphology correlates with JPS genotype, and assess the utility of morphometric analysis in JPS.

Methods: The study cohort included JPS patients consented for research on our IRB-approved protocol. We searched the pathology archives at our institution for all available H&E slides from polypectomy specimens for these patients. All subjects underwent clinical SMAD4 and BMPR1A sequencing, deletion, and duplication analysis and research whole exome sequencing (WES). Polyp morphology was assessed by two pathologists blinded to patient identity and genotype, and each polyp classified into one of five categories (classic JP, epithelial JP, indeterminate JP, incipient JP, non-JP polyp). A representative subset of polyps was morphometrically assessed for relative stromal/epithelial composition by grid point counting. Data were then unblinded and correlated to genotype.

Results: Approximately 250 polyps were assessed from 38 patients (4 BMPR1A mutation, 3 SMAD4, 1 each of proposed candidate drivers identified in WES: SMAD7, BMPR2, LTBP2). Overall polyp morphology was heterogenous (~160 classic JP, ~10 epithelial JP, 45 indeterminate JP including 27 gastric polyps in two SMAD4 patients, 31 incipient JP, 9 non-JP polyps). Low-grade dysplasia was rare (<5% of polyps); no high-grade dysplasia was identified. The majority of colonic polyps in all genotypes were classic JP. Excluding incipient polyps, 11/38 patients had multiple polyp types, including 5 different polyp types in the BMPR2 patient. Morphometric analysis of 101 polyps from 35 patients showed 16 stroma-poor (<50%) colonic polyps, 12 of which were classic JP.

Conclusion: In contrast to a prior study, we found the majority of colonic polyps in JPS patients have classic morphology, regardless of genotype. The distinction of JP into classic and epithelial morphology is somewhat artificial with intermediate forms. A substantial minority of JPS patients have morphologically heterogenous polyps, including non-JP polyps. BMPR2 mutation may predispose to multiple polyp types. Morphometric analysis adds little to morphologic assessment of polyps in JPS.

12

Focal Nodular Hyperplasia-Like Lesions with Glypican-3 Positivity: A Potential Mimicker for Hepatoblastoma

L Berklite[1], A Shenoy[2], M Hollowell[3], B Fung[2], S Ranganathan[1]; [1]Cincinnati Children's Hospital Medical Center, Cincinnati, Ohio; [2]Nationwide Children's, Columbus, Ohio; [3]Boston Children's Hospital, Boston, Massachusetts

Background: Glypican-3 is often used to discriminate between neoplastic and non-neoplastic liver, and positivity may be considered supportive of malignancy. However, glypican-3 is also normally expressed in immature liver. We present 5 cases of focal nodular hyperplasia (FNH)-like lesions with glypican-3 expression arising in infants and highlight the challenges these lesions present in the differential diagnosis of hepatoblastoma.

Methods: Five cases were obtained from the files of three pediatric hospitals. Pertinent data including presentation, imaging, AFP levels, and outcome were obtained from the medical record. H&E slides and immunohistochemical stains for glypican-3, beta-catenin, CD34, glutamine-synthetase, reticulin, and GLUT-1 were reviewed.

Results: Clinical and imaging features are summarized in Table 1. Microscopically, all cases showed variably demarcated hepatocellular lesions with trabecular architecture (2-4 cells thick) and marked sinusoidal dilatation. Well-defined portal tracts were not readily identified. Two cases had fibrous areas containing bile ducts. Cytologic atypia was absent and mitotic activity was low. All lesions showed glypican-3 expression without nuclear beta-catenin (Table 1). CD34 was positive in sinusoids in 4/5 cases. After biopsy, 1/5 patients underwent resection while 2/5 underwent observation only.

Table 1. Clinical Features and Immunophenotype

Case	Age	Sex	Size(cm)	Presentation	Peak AFP (ng/mL)	Other conditions	Imaging impression	Glypican 3	Beta-catenin
1	2wk	M	8.1	Incidental	204,696		Infantile hemangioendothelioma v. HB	Granular canalicular(L)	M
2	4mo	F	0.9	Incidental	317	Hypoplastic aortic arch; muscular VSD	Hemangioma, FNH, mesenchymal hamartoma, HB	Canalicular(L,B)	M
3	6mo	F	1.8	Incidental	88.6		HB v. congenital hemangioma	Granular(L,B)	M
4	9wk	M	2.4	Incidental	1972	Horseshoe kidney, dysplastic L renal moiety	FNH v. HB	Weak/Moderate(L,B)	M
5	2mo	M	4.2	Incidental	43,097	R aortic arch, bladder	Congenital hemangioma	Granular(L,B)	M

						outlet obstruction, central apnea			

HB-hepatoblastoma; M-membranous; L-lesion; B-Background

Conclusion: Our study highlights the pitfalls of evaluating liver lesions in infants when high AFP levels and glypican-3 expression may be a reflection of immaturity rather than evidence of neoplasia. In these patients, FNH-like lesions can be a strong mimicker for hepatoblastoma and must be carefully evaluated. An underlying cardiac or vascular flow abnormality may be a predisposing factor for these mimics.

13

Clinicopathologic Characterization of Lymphocytic Colitis in the Pediatric Population

I Gonzalez, T Patel, M Conrad, J Kelsen, S Weinbrom, P Russo; Children's Hospital of Philadelphia, Philadelphia, Pennsylvania

Background: Lymphocytic colitis (LC) is typically seen in older females with watery diarrhea and a normal colonoscopy. Only limited case series have been reported in the pediatric population which have suggested an association with immunodeficiencies, medications and inflammatory bowel disease (IBD). In this study, we sought to characterize the clinicopathologic features of LC in the pediatric population.
Methods: A search was performed from 1/2000-10/2021 for LC. All cases were reviewed blinded from the clinical information. Increase IELs was defined as >20 lymphocytes per 100 enterocytes throughout the GI tract. Lamina propria eosinophils were counted in one HPF (0.063 mm) in a hot-spot area. Clinical response was defined as resolution of symptoms.
Results: 61 LC cases were identified with a median age of 13 yrs (2.4–18); 18% presented in patients <6 yrs, 21% between 6 to 12 yrs and 61% between >12 to 18 yrs. There was a female predominance overall (72%), except in those <6 where 55% were male. Abdominal pain and diarrhea were the most common symptoms (75%). 39% and 15% of patients had allergies (food, medications, and food and medication allergies in 54%, 21% and 8%, respectively) and celiac disease (CD), respectively. Most patients with CD also had terminal ileum with IELs. An immunodeficiency was present in 8.5% of the patients including two patients <6 yrs. 88% of the patients were not taking any medications at the time of procedure. Upper endoscopy (n=58) showed a normal esophagus (91%), stomach (88%) and duodenum (83%), with the most common pathology being eosinophilic esophagitis (5%), chronic inactive gastritis (5%) and duodenal IELs without villous blunting (10%). Terminal ileum biopsies (n: 54) were commonly normal (70%) and in 26% of them IELs were seen. The median number of IELs in the right colon (n: 39), left colon (n: 43) and random colon (n: 18) were 47 (28–85), 45 (24–78) and 39 (25–75), and of lamina propria eosinophils were 24 (7–62), 14 (5–40) and 21 (12–66); respectively. Neutrophilic and eosinophilic cryptitis were detected in 16% and 10% of cases, respectively. Crypt apoptosis was identified in 52% of cases and were most common in patients <6 yrs (91%) (p=0.017). Mean clinical follow-up time was 28.5 months. Clinical response was seen in 63% of patients. Patients without clinical response were commonly <6 yrs (56%) (p=0.036) and were associated with a higher IELs (median: 52 vs 38, p=0.032). The clinicopathologic features by patients age groups are summarized in Table-1.

Table 1. Clinicopathologic characteristics of lymphocytic colitis by patient age groups (N = 61)

	< 6 years (n: 11)	6 – 12 years (n: 13)	12 – 18 years (n: 37)	*P*
Gender, n, %				
Male	6, 54.5%	3, 23.1%	8, 21.6%	0.092
Female	5, 45.5%	10, 76.9%	29, 78.4%	
Allergies, n, %				
Yes	5, 50.0%^	3, 23.1%	15, 40.5%	0.381
No	5, 50.0%^	10, 76.9%	22, 59.5%	
Underlying immunodeficiency, n, %				
Yes	2, 20.0%^	1, 7.7%	2, 5.6%[&]	0.347
No	8, 80.0%^	12, 92.3%	34, 94.4%[&]	
Celiac disease, n, %				
Yes	2, 20.0%^	2, 15.4%	5, 13.9%[&]	0.893
No	8, 80.0%^	11, 84.6%	31, 86.1%[&]	
Inflammatory bowel disease, n, %				
Yes	0, 0%^	0, 0%	5, 13.9%[&]	0.175
No	10, 1000%^	13, 100%	31, 100%[&]	
Clinical response, n, %				
Yes	4, 44.4%[#]	12, 92.3%	20, 57.1%[&]	**0.036**
No	5, 55.6%[#]	1, 7.7%	15, 42.9%[&]	
Esophagus, n, %				
Normal	9, 90%^	11, 84.6%	33, 94.3%[$]	0.416
Lymphocytic esophagitis	1, 10%^	1, 7.7%	0, 0%[$]	
Eosinophilic esophagitis	0, 0%^	1, 7.7%	2, 5.7%[$]	
Stomach, n, %				
Normal	10, 100%^	12, 92.3%	29, 82.9%[$]	0.889
Chronic inactive gastritis	0, 0%^	1, 7.7%	2, 5.7%[$]	
Chronic mild active gastritis	0, 0%^	0, 0%	1, 2.9%[$]	
Lymphocytic gastritis	0, 0%^	0, 0%	1, 2.9%[$]	
Reactive gastropathy	0, 0%^	0, 0%	2, 5.7%[$]	
Duodenum, n, %				
Normal	7, 70%^	10, 76.9%	31, 88.6%[$]	0.634
Increase IELs without villous blunting	1, 10%^	1, 7.7%	2, 5.7%[$]	
Villous blunting and increased IELs	2, 20%^	2, 15.4%	2, 5.7%[$]	
Terminal ileum, n, %				
Normal	4, 80%[@]	8, 66.7%[!]	26, 70.3%	0.939
Increase IELs	1, 20%[@]	4, 33.3%[!]	9, 24.3%	
Active ileitis	0, 0%[@]	1, 7.7%[!]	1, 2.7%	
Poorly formed granuloma	0, 0%[@]	0, 0%[!]	1, 2.7%	
IELs number per 100 enterocytes, median, range	61, 29 – 72	47, 28 – 75	52, 25 – 85	0.776
Neutrophilic cryptitis, n, %				
No	8, 72.7%	9, 69.2%	34, 91.9%	0.174
Yes	3, 27.3%	4, 30.8%	3, 8.1%	
Lamina propria eosinophils per HPF, median, range	30, 6 – 49	31, 12 – 52	23, 7 – 66	0.846
Eosinophilic cryptitis, n, %				
No	9, 81.2%	12, 92.3%	34, 91.9%	0.589
Yes	2, 18.2%	1, 7.7%	3, 8.1%	
Crypt apoptosis, n, %				
No	1, 9.1%	8, 61.5%	20, 54.1%	**0.017**
Yes	10, 90.9%	5, 38.5%	17, 45.9%	
Number of crypt apoptosis in 10 contiguous crypts, median, range	3, 0 – 5	2.5, 0 – 4	2, 0 – 11	0.303

Abbreviations: IELs – intraepithelial lymphocytes; HPF – high power field.
Only available in: ^10, [&]36, [#]9, [$]35, [@]5 and [!]12 patients.
Percentages might not add to 100 due to rounding.

Conclusion: We present the largest pediatric cohort of LC to date. The most common associated comorbidity was a history of allergies (39% of cases). Surprisingly, many of the patients failed to have symptomatic improvement and these cases were associated with higher IELs at the time of diagnosis.

PLATFORM III: Perinatal

14

Placental Interferon Signaling is Involved in Chronic Intervillositis of Unknown Etiology
J Terry; BC Children's Hospital, Vancouver, British Columbia

Background: Chronic intervillositis of unknown etiology (CIUE) is a recurrent placental inflammatory process associated with early pregnancy loss. The etiology of CIUE is unclear but may involve infection or aberrant maternal immune response. Evaluation of inflammatory signaling by placental villus stroma, cyto/syncytiotrophoblast, and maternal macrophage in CIUE may reveal the underlying mechanism(s) of macrophage recruitment and placental damage. The objective of this study is to assess CIUE inflammatory signaling by whole transcriptome expression analysis using digital spatial profiling (DSP).
Methods: Ethics approval is obtained to compare formalin-fixed paraffin embedded placental tissue from high grade CIUE (4 cases, average gestational age 11 weeks) to control normal placenta (NP; 4 cases, average gestational age 11 weeks) and granulomatous lymphadenitis (GLA) as a macrophage inflammation control (4 cases). A microarray of representative tissue from each case is constructed for DSP. CD68 and cytokeratin highlight macrophage and trophoblast to delineate the following tissue areas of interest for analysis: CIUE trophoblast, NP trophoblast, CIUE stroma, NP stroma, CIUE maternal macrophage, and GLA macrophage. Principal component analysis (PCA), gene expression analysis by unpaired t-test, and Gene Set Enrichment Analysis (GSEA) are used to compare CIUE tissues to relevant controls.
Results: One GLA macrophage control does not meet quality criteria and is excluded from analysis. PCA demonstrates clustering of each tissue type with more variability in CIUE trophoblast and stroma. Gene expression analysis shows overexpression of interferon (IFN)-induced genes in CIUE trophoblast (HLA-DPB1, IDO1) and fatty acid metabolism-related genes in CIUE macrophage (e.g. CD36, OLR1). GSEA shows prominent enrichment in IFNγ, IFNαβ, IL-4/IL-13, PD1, and IL-10 signaling pathways in both CIUE trophoblast and stroma. There is no significant difference between CIUE and GLA macrophage inflammatory pathways, suggesting a similar inflammatory phenotype.
Conclusion: DSP with whole transcriptome expression analysis identifies prominent IFN singling in CIUE stroma and trophoblast implying placenta drives CIUE. The roles IFNs play can be variable and contextual but one interpretation is IFNγ signaling occurs in response to pattern recognition receptor activation by cytoplasmic bacterial components or foreign nucleic acids and lowers macrophage sensitivity to anti-inflammatory mediators, which may explain the prominence of IL-4/IL-13, PD-1, and IL-10 signaling pathways without apparent effect. The role of IFNαβ may represent reaction to prolonged IFNγ signaling but could also be a response to viral infection. Further study of IFN signaling in CIUE will lead to better understanding of this disease.

15

Pathogen-Specific Nucleic Acid Targets in Umbilical Cord Tissue: Correlations with Neonatal Blood Culture And Placental Histology

*A Freedman[1], K Mangold[2], E Price[2], L Ernst[2]; [1]*Northwestern University, Evanston, Illinois; [2]NorthShore University HealthSystem, Evanston, Illinois

Background: Despite advances in prenatal care, infection acquired in utero leading to early onset neonatal sepsis (EOS) remains a leading cause of infant morbidity and mortality worldwide. Growth of an infectious pathogen in infant blood is the current gold standard for diagnosis of EOS, but has a low sensitivity in neonates due to maternal antibiotic treatment, small specimen volumes, and low-grade bacteremia. Our aim was to develop more sensitive laboratory testing for EOS by using umbilical cord tissue from the placenta and applying molecular methods seeking pathogen-specific RNA transcripts.
Methods: Selected neonates born between 2017-2020 with a blood culture drawn within the first 72 hours of life were included. Total RNA was extracted from formalin fixed paraffin embedded umbilical cord tissue. A custom Nanostring panel was designed to target 31 RNA transcripts from bacterial and fungal species, and transcripts were quantified using the NanoString nCounter System. We determined whether a bacterial species was present by identifying outliers using the interquartile range (IQR) method; bacterial species with expression values at least 3 IQRs above the third quartile were considered to be present in the sample. A sample was considered positive for a pathogen if at least one of the 31 targets was identified as an outlier. Placenta pathology was categorized in four domains: acute inflammation (AI), chronic inflammation (CI), fetal vascular malperfusion (FVM) and maternal vascular malperfusion (MVM). We used Fisher's exact test to compare the prevalence of placental pathology among those with and without pathogen-specific transcripts detected by NanoString.
Results: 96 neonates were included, 14 (15%) with positive blood culture and 82 (85%) with negative blood culture. One specimen in the negative blood culture group was excluded from analysis due to technical failure. Mean gestational age was 36.2 weeks (range 22-42 weeks). Overall, 53/95 (56%) umbilical cords were identified as positive based on NanoString, and 10/14 (71%) with positive blood cultures were classified as positive. Universal bacterial 16S rRNA (n=22) and Ureaplasma (n=18) were the most frequently identified transcripts. High grade AI was twice as common among those identified as positive based on NanoString (54.7% vs. 28.6%; p=0.01). The placenta showed fetal AI in 56/95 (59%), and high grade fetal AI was present in 43.4% of positive samples and only 16.7% of negative samples ($p<0.01$).
Conclusion: Molecular techniques using umbilical cord tissue to detect pathogen-specific RNA transcripts reveal many more potential bacterial species than neonatal blood culture alone. These findings may be important for understanding amnionic fluid infection and its effect on the neonate. Further study is required.

16

Parental Experiences of Perinatal Autopsy: A Mixed Methods Study

K Hanson[1], D Côté-Arsenault[2], S Hawsawi[2], S Besmer[1]; [1]Saint Louis University School of Medicine, St. Louis, Missouri; [2]Trudy Busch Valentine School of Nursing, Saint Louis University, St. Louis, Missouri

Background: This study aims to understand parental satisfaction with perinatal autopsy. Autopsies can help provide a sense of closure to bereaved parents, help them better understand the cause of their baby's death, and in some cases, help prevent future losses. Greater understanding about the cause of perinatal loss has been shown to help bereaved parents cope with perinatal loss. Limited literature indicates a level of parental dissatisfaction with the autopsy experience. There is a need for increased data about how families of decedents experience the autopsy process and review and perceive the resulting autopsy reports.

Methods: A mixed methods design was utilized. Parents whose baby had an autopsy at the site institution between 2018 and 2020 were invited by mail and email to complete on an online survey then were given an opportunity to participate in a video conference interview. A database was drawn from electronic health records and 99 potential participants met study criteria. Survey data was analyzed using descriptive statistics. Quantitative and qualitative data were integrated for thematic analysis.

Results: 17 participants completed the survey and 7 were interviewed. 43.8% of participants felt the process of autopsy was fully explained before they consented to the procedure; 31.3% felt that they were given some information and 25% felt that that they were given no information. 62.5% of parents reported satisfaction with the amount of information they were given about the autopsy process while 37.5% reported dissatisfaction. Only 6.7% of participants felt that autopsy helped them process their baby's death; 53.3% felt it helped somewhat and 40.0% felt it was unhelpful. Overall satisfaction with the autopsy process ranged from 26.6% reporting unsatisfied or little satisfied to 73.5% reporting somewhat to very satisfied.

Conclusion: Communication with the health care system was identified as an area needing improvement. It is important to appropriately set expectations for parents about the type of information that can be gained by autopsy and the timeline of the autopsy procedure and results. Some bereaved parents reported that the autopsy reports were not explained to them by their physician. There is a need to ensure adequate follow up with clinicians. Additionally, it is recommended that autopsy reports be written using language that is accessible to lay people. Overall, there was satisfaction with the autopsy process however utility would be improved with greater communication within the healthcare system, setting appropriate expectations, attention to accessibility of language, and guidelines to ensure adequate follow up.

17

C4d immunostaining in the Placentas of Women with Chronic Intervillositis of Unknown Etiology

E Chan[1], L de Koning[1], W Yu[1], R Chadha[2]; [1]University of Calgary, Alberta Children's Hospital, Calgary, Alberta; [2]University of Calgary, Calgary, Alberta

Background: Chronic intervillositis of unknown etiology (CIUE) is characterized by mononuclear cell infiltrates in the placental intervillous space. CIUE is associated with adverse pregnancy outcomes and a high recurrence rate, and is likely related to a maternal alloimmune response. In 2015, Bendon et al found that a high proportion of placentas with CIUE had extensive C4d staining of the syncytiotrophoblasts. C4d, a degradation product of the classic complement pathway, can indicate antibody-mediated rejection in organ transplantation. Benachi et al (2021) found high levels of complement-fixing, fetus-specific, anti-human leukocyte antigen antibodies among 2 women with recurrent CIUE-associated pregnancy losses after a first normal pregnancy. Immunomodulatory therapies may prevent recurrence. The goal of this study was to examine C4d staining in placentas of women with ≥ 1CIUE-associated pregnancy loss. Specifically, we examined placentas with CIUE from autopsy cases, previous placentas and subsequent placentas, including those post-immunomodulatory therapy.

Methods: This was a retrospective study of fetal autopsy cases associated with CIUE from 2017-2021. We identified CIUE-associated fetal demises (index cases), from our autopsy database. We then reviewed all available placental slides (before and after index case), and performed C4d immunostaining on 1 representative section from each placenta. C4d staining of the syncytiotrophoblasts was graded as: 0+ = <5%; 1+ = 5 to <25%; 2+ = 25 to <75%; 3+ ≥75%. Maternal and fetal characteristics were also reviewed.

Results: We found 5 CIUE-associated fetal autopsy cases, from 5 women. Of the 5 women, 3 had a primigravida placenta (prior to index case) available for examination: 1 had a stillborn associated with CIUE and 3+ C4d staining, and the other 2 each had a term liveborn without CIUE, but 3+ C4d staining. These 2 women had subsequent fetal losses associated with CIUE, with 3+ C4d staining. Of the 5 women, 3 had immunomodulators (e.g. intravenous immune globulin, hydroxychloroquine, prednisone) after CIUE-associated pregnancy losses. Following treatment, 1 woman had a 37-week liveborn, without CIUE or C4d staining (0+). The second woman had a 35-week liveborn, with chronic villitis, mild CIUE, and 1+ C4d staining. The third woman had a stillborn at 25 weeks with CIUE, but milder 2+ C4d staining compared to previous pregnancies (3+ C4d).

Conclusion: Diffuse C4d staining of syncytiotrophoblasts can be observed in the first “normal” placentas of women who develop CIUE in future pregnancies. This suggests that complement-fixing antibodies might be present in maternal blood in the first uncomplicated pregnancy. Also, our study suggests that immunomodulatory treatment may help prevent CIUE recurrence by downregulating the classical complement pathway.

18

Craniolacunia and the Development of the Fetal Calvaria: An Autopsy Series With Clinical and Histological Analysis

R Reed; Seattle Children's Hospital, Seattle, Washington

Background: Craniolacunia, also known as lückenschädel, is a congenital abnormality of the calvaria featuring well-circumscribed, round or oval areas of marked thinning on the inner skull table, interspersed with more-normal bone. It is usually identified in third trimester fetuses and newborns, and usually resolves by 3-6 months. Craniolacunia is best seen on X-ray of the skull, and is rarely identified in the modern era. It is commonly associated with myelomeningocele and/or Chiari 2 malformation and very rarely described in patients lacking CNS abnormalities. A single previous autopsy series and description of histology was published in 1948.

Methods: Records and photographs were reviewed from 13 autopsy cases with craniolacunia. In 5 cases, histologic sections of involved calvaria were available. To investigate normal calvarial development, 23 parietal bone samples from fetuses/infants of 16-42 weeks gestation were examined. Variables recorded included thickness of bone, extent of osteoblastic rimming, and architecture.

Results: Normal parietal bone development had reproducible morphologic stages in the second and third trimesters. Bone thickness increased with gestational age, while osteoblast numbers decreased. Craniolacunia was mainly seen in term neonates, although still present in a few older patients. Five of the 13 patients had Chiari 2 malformation, one had hydrocephalus, and two had other structural CNS abnormalities. One had trisomy 18. Four had no congenital abnormalities. Two sustained intrapartum skull fractures through lacunae. Lacunae in term infants comprised areas of marked thinning (11-27% the thickness of adjacent bone) with distinctly immature architecture, histologically similar to normal calvaria at 16-20 weeks. Adjacent bone was normal to slightly reduced in thickness, with age-appropriate architecture but increased osteoblast numbers.

Conclusion: This is the largest autopsy series of craniolacunia ever presented, and the first systematic histologic analysis of craniolacunia and the developing fetal calvaria. The association with CNS abnormalities, including myelomeningocele, Chiari 2, porencephaly, and a calvarial defect with exposed cerebral hemispheres, supports the hypothesis that decreased CSF pressure and ventricular distention promote craniolacunia development. In light of emerging evidence that both dura and dermis are sources of signals that drive osteoblastic differentiation, perhaps ventricular distention is needed to keep these tissue layers approximated and induce timely induction of osteoblasts. In the setting of reduced CSF pressure, it is possible that osteoblastic differentiation is delayed, leading to the histologic appearance in craniolacunia of immature bone and increased osteoblastic rimming, the latter both in lacunae and throughout the calvaria.

19

Pre-conception SARS-CoV-2 PCR+ in Women affects Pregnancy Outcome and Placental Pathology

P Hernande, L Chen, Y Ma, R Zhang, R Jackups, L Dehner, D Nelson, M He; Washington University in St. Louis School of Medicine, St. Louis, Missouri

Background: Whether the timing of maternal SARS-CoV-2 infection influences placental histopathology or pregnancy outcome is debated. We tested the hypothesis that the time peri-pregnancy when a woman tests SARS-CoV-2 PCR+ influences placental pathology and pregnancy outcomes.

Methods: We conducted a retrospective, case-control study of obstetrical charts in the EPIC medical record between April 1, 2020 and September 22, 2021. Maternal SARS-CoV-2 PCR results were identified from EPIC, and placental pathology reports and histopathology slides were retrieved from the Department of Pathology database (CoPath) and centrally reviewed by a board certified pediatric pathologist blinded to clinical history. Patients testing PCR+ for SARS-CoV-2 were classified into four groups: pre-conception during the study period (G0), in the 1st (G1), 2nd (G2), or 3rd (G3) trimester of pregnancy. A fifth group (GC) served as control pregnancies, who tested negative and delivered a singleton newborn in the 3rd trimester. One-way ANOVA compared continuous variables, and Chi-square or Fisher exact test were used for categorical variables. $P < 0.05$ was significant.

Results: Seventy one pregnancies were studied, including 19 that were PCR- in the 3rd trimester (GC) and 52 that were maternal SARS-CoV-2 PCR+. Among those testing positive, 11 were PCR+ before pregnancy (G0), 8 were PCR+ in the 1st trimester (G1), 16 were PCR+ in the 2nd trimester (G2) and 17 were PCR+ in the 3rd trimester (G3). The table summarizes the outcomes.

Parameter	A	B	Statistic	P
Accelerated villous maturity	G0:5/7(71.4%) G1:5/7(71.4%) G2:7/15 (46.7%)	G3: 3/17 (17.6%) GC: 2/19 (10.5%)	Chi-square Fisher exact	0.002
Chronic chorioamnionitis	G1: 2/7 (28.6%)	Other groups: 0%	Chi-square	0.001
Pregnancy loss < 20 weeks GA	G0: 4/11 (36.4%)	Other groups: 0%	Chi-square	0.001
Neonatal death	G0: 2/7(28.6%)	Other groups: 0%	Chi-square	0.02
Birth weight difference (g)	G0: -1,001	G2	One-way ANOVA	0.02
	G0: -893	G3	One-way ANOVA	0.02
Gestational age at delivery(d)	G0: -11	G2 G3	One-way ANOVA	0.000

[1]Statistic tested each group listed in cell of column A to each group in cell of column B.

Conclusion: Our single institution experience confirms our hypothesis. Notably, maternal infection with SARS-CoV-2 before pregnancy has the greatest impact on adverse outcomes, compared to maternal positivity during pregnancy or in women who test PCR negative during the 3rd trimester.

POSTERS

20

Utility of Cytogenetics in New Pediatric Leukemia Diagnosis at An Era of Next Generation Sequencing

A Kaur, A Richardson, S Gong; Northwestern University, Chicago, Illinois

Background: Molecular studies are a part of routine diagnostic workup for many of the cancers especially hematologic malignancies. It is used to predict prognosis and responses to targeted therapies. With the widely available new molecular techniques nowadays including next generation sequencing (NGS), the importance of routine cytogenetics including fluorescent in situ hybridization (FISH) and karyotyping is uncertain.

Methods: We retrospectively reviewed all newly diagnosed cases of acute leukemia, myelodysplastic syndrome (MDS), and MDS/myeloproliferative neoplasms (MDS/MPN) from April 2019 to September 2021. It included 72 pediatric patients in the age range of 0-18 years. It included 49 cases (68%) of B-cell lymphoblastic leukemia/ lymphoma (B-ALL), 11 cases (15%) of Acute myeloid leukemias (AML), 7 cases (10%) of T-cell lymphoblastic leukemia/ lymphoma (T-ALL), 2 cases of mixed phenotype acute leukemias, 2 cases of MDS/MPN and 1 case of MDS with fibrosis. Morphologic and flow cytometric data were reviewed on all these cases. Routine cytogenetics was available in 69 cases (96%) and NGS panel (Pediatric Oncomine) was available in 68 cases (94%).

Results: We found that cytogenetics and NGS contributed to initial diagnosis in 87% of cases and 91% of cases respectively. Among the 65 cases with both cytogenetics and NGS data available, cytogenetic data is indispensable for establishing the diagnosis in 26 cases (40%). We subdivided these cases into the following 3 categories: First category included cytogenetics that provided copy number changes of chromosomes which are not validated on NGS and these accounted for 77% of these cases. Second category included some rearrangements including CRLF2, MECOM and MYC which were only detectable by FISH because they were not covered by NGS. This category included 15% cases. The third category included cytogenetics which helped to satisfy the WHO diagnostic criteria. This category had MDS and MDS/ MPN cases (8% overall). For the remaining cases (60%), cytogenetics provided duplicated results or confirmed the NGS results but did not provide new data, therefore theoretically replaceable.

Conclusion: As the NGS based tests gain wide acceptance, our study showed that cytogenetics was irreplaceable in 40% of new acute leukemia, MDS, and MDS/MPN diagnosis which is a significant number of cases. We suggest that cytogenetics still plays an important role in diagnosis of new hematologic malignancies and is irreplaceable in at least pediatric population.

21

The Utility of Intraoperative Frozen Section Evaluation for Margin Status in Surgical Management of Pediatric Cutaneous and Soft Tissue Fungal Infections

B DePasquale, R Linn; Children's Hospital of Phildelphia, Philadelphia, Pennsylvania

Background: Invasive fungal infections are an important cause of morbidity and mortality in immunocompromised children. Deep cutaneous infections, though less common than pulmonary and rhino-cerebral disease, are similarly life-threatening. Treatment involves a combination of systemic antifungal therapy and surgical debridement, ideally with healthy margins. Some institutions use intraoperative frozen section (FS) to obtain clear margins during surgical debridement; however, there is limited data published about the utility of FS in these cases. The goal of this study is to determine the frequency, source, and clinical outcome of discrepancies between FS and permanent section (PS) of margins for cutaneous fungal infection excisions.

Methods: All excisions performed for cutaneous fungal infections at a tertiary care children's hospital over an 18-year period (2003-2021) were reviewed retrospectively to identify cases in which FS for margin assessment were performed. The diagnosis from the final surgical pathology report was compared with each FS diagnosis and were classified as concordant or discordant. Discordant results were further classified as due to a sampling error (fungal organisms present within the frozen tissue but not present on the FS slide) or interpretation failure (undercalls or overcalls at the time of FS). The clinical impact of the discordant results was categorized as either: minor (minimal or no increased risk to patient, i.e. additional surgical margins at time of initial surgery) or major (increased risk of harm to patient, i.e. requiring additional surgery).

Results: A total of 30 cases with 96 pairs of FS and PS diagnoses from 25 patients were reviewed. Discordance was found in 7 pairs (7.3%). In 5 pairs (5.2%), discordance was due to a sampling error, whereby the fungi were only identified on PS, yielding a false negative. In most of these pairs, the fungi were present within the subcutaneous adipose tissue, which is notoriously difficult to cut on frozen section. All results had a major clinical impact on patients, leading to a repeat surgery for re-excision or biopsy. In 2 pairs (2.1%), there was an interpretation failure with overcalls at the time of FS (false positive) resulting in minor clinical impact. Overall, the accuracy of FS margin evaluation for fungi was 93%. The sensitivity and specificity were 72% and 97%, respectively.

Conclusion: Surgical debridement with clean margins is an integral part of treatment for cutaneous fungal infections. While specific, FS margin assessment for these cases suffers from a lower sensitivity that may lead to repeat surgeries. Sampling errors were the most common cause and may be explained by the fatty nature of these specimens, which must be taken into consideration when making intraoperative diagnoses.

22

NUTM1 Fusion in a Biphasic Pulmonary Blastoma and a Primary Hepatobiliary Carcinoma

J Slack, L Teot, A Perez-Atayde, S Vargas; Boston Children's Hospital/Harvard University, Boston, Massachusetts

Background: NUTM1 fusion is a hallmark of NUT carcinoma, an undifferentiated carcinoma often containing foci of abrupt squamous differentiation. NUTM1 fusion has been recently identified in an expanding array of tumors, including salivary gland-type neoplasm with pleomorphic adenoma-like features, cutaneous adnexal tumor, germ cell-like tumor, and undifferentiated sarcoma. These tumors have diverse clinical, histologic, and molecular features distinguishing them from classic NUT carcinoma. We report 2 novel cases that further expand the spectrum of NUTM1-rearranged tumors.

Methods: Clinical, histologic, immunohistochemical, and molecular features of two unique NUTM1-rearranged tumors were examined.

Results: Case 1. This 13-year-old girl with a 6 week history of cough, fever, chest pain, and worsening left lung consolidation presented with a 9-cm left lower lobe mass and mediastinal lymphadenopathy. Needle biopsy showed microcysts lined by bland cuboidal to columnar epithelial cells, along with subjacent collections of poorly differentiated mesenchymal cells with large vesicular nuclei, prominent nucleoli, exuberant neutrophilic infiltrate, and patchy necrosis. Epithelial cells stained for cytokeratins, EMA, CEA, and TTF-1; mesenchymal cells stained for SMA and, faintly, TTF-1, S100, and CD99; both stained for β-catenin (nuclear and cytoplasmic) and NUT. FISH identified a BDR4-NUTM1 fusion. Targeted next-generation sequencing (NGS) confirmed BRD4 (exon 16) as the fusion partner. The pathologic findings were consistent with a NUTM1-rearranged pulmonary blastoma. Ten days post biopsy, the tumor had grown into the heart and diaphragm and metastasized to bone and brain. Four months post biopsy, after palliative chemotherapy, the patient died of disease. Case 2. A 16-year-old girl with several weeks of abdominal symptoms presented with a 25-cm liver mass and extensive bone and lymph node metastases. Needle biopsy showed epithelioid and polygonal to columnar cells in solid, cribriform, and tubuloacinar arrangement within desmoplastic stroma. Cytoplasm was ample and eosinophilic to clear. Nuclei were round with small nucleoli. The tumor was positive for cytokeratins, NUT, p63, CEA, and Hep-Par1. FISH revealed NUTM1 rearrangement without involvement of BRD4. Partial NUTM1 and NSD3 copy losses on targeted NGS were consistent with NSD3-NUTM1 fusion. The pathologic findings were consistent with a NUTM1-rearranged hepatobiliary carcinoma. The patient received palliative chemotherapy and died of disease 14 months after diagnosis.

Conclusion: Our findings demonstrate that pulmonary blastoma and hepatobiliary carcinoma are among the NUTM1-rearranged tumors that can occur in young patients and exhibit aggressive behavior.

23

Somatic Copy Number Alterations and Mutation Landscape in Malignant Rhabdoid Tumor

Y Ma, M Kaushal, L Dehner, J Pfeifer, M He; Washington University in St. Louis, St. Louis, Missouri

Background: Malignant rhabdoid tumors (MRT) are aggressive malignancy that predominantly affects infants and young children. MRTs are driven by pathogenic variants of SMARCB1/INI1 or rarely SMARCA4. Our hypothesis was, that tumor heterogeneity suggested, in addition to the driver mutation(s), other genomic alterations in MRT might contribute to tumorigenesis, tumor progression including metastasis, and response to treatment. This study aimed to study genomic alterations in addition to the driver mutations in MRT.

Methods: With IRB approval, normal-tumor paired whole exome sequencing (WES) were performed in five cases which had sufficient amount of both normal and tumor tissue, some with both primary and relapsed/metastatic tumors. In these five cases, all had primary tumor. Three cases with post-treatment samples. Sequencing targeted 25-30M reads for normal tissue and 45-50M reads for neoplastic tissue. Mutation (variation) analysis and somatic mutation discovery for single nucleotide variants (SNVs) was performed using MuTect v1.1. Copy number alterations was determined by comparing the aligned number of reads per gene generated by WES in tumor with those in normal tissue control by cn.mops. mRNA sequencing and immunohistochemistry were also applied to compare with WES findings.

Results: Our study revealed several recurrent somatic copy number alterations which harbor genes which alterations were reported to be involved in malignancy, including 2q37.3 gain (4/5, 80%, TWIST2), 7q32.1 gain (3/5, 60%), 11q12.2 gain (3/5, 60%), 14q32.3 gain (4/5, 80%), 19p13.2 loss harboring SMARCA4 (2/5, 40%), 21q22.3 gain (3/5, 60%), and 22q11.1 loss (2/5, 40%) involving SMARCB1. Alterations more seen in post-treatment MRT included 11p15.4 gain (3/3, 100%) and 11q12.2 gain (2/3, 67%). A few somatic copy number variations are only seen for posttreatment MRT patients, including LMO1, MMP26, TRIAP1, TRAF3 and SLC9A3R1. Above results were compared with available IHC and RNA results.

Conclusion: Overall, our study revealed that in addition to the driver mutations, there were recurrent genomic alterations in MRT. Those somatic copy number alterations are associated with genes involved in tumorigenesis include SMARB1, SMARCA4, TWIST2, TRIAP1, MTA1 and XIAP. A few somatic variations are only seen for posttreatment MRT tumors, including LMO1, MMP26, TRIAP1, TRAF3 and SLC9A3R1. Gain of 11p15.4 is the only recurrent somatic copy number alteration in two metastatic cases. This is the first study to report the specific somatic copy number variations in posttreatment MRT patients.

24

Alpha-1-Antitrypsin Deficiency Associated Venous Thrombosis in Children

L Goetz[1], K Patel[2]; [1]Houston Methodist Hospital, Houston, Texas; [2]Texas Children's Hospital, Baylor College of Medicine, Houston, Texas

Background: Recent reports have shown increased risk of venous thrombosis (VT) in adult carriers and patients of alpha-1-anti trypsin deficiency (A1AT) with a Z allele; through liver disease or effects on coagulation factors. This study aims to review the pre and post-transplant course of children undergoing liver transplant (LT) for A1AT with a focus on thromboembolic events and venous findings in the explant.
Methods: With appropriate IRB approval, liver explants of A1AT were identified from the pathology database from 2002-2021. Medical records were reviewed along with all available explant slides in a retrospective manner.
Results: Eight children with A1AT were identified, 4 females, with age at LT ranging from 7 months to12 years (median 1.5 years). Five (62.5%) had the homozygous Pi ZZ genotype, two (25%) Z/null genotype, and one (12.5%) unknown. Lung disease was present in three patients (37.5%). There were no records of pre-transplant VT in any patient, but post-transplant VT was seen in 6 (75%) involving portal vein in 4, junction of right hepatic vein and IVC in 1, and basilic vein in 2. Explants of 3 of the 4 patients with post-transplant portal VTE showed organizing thrombi and variable intimal fibromyxoid hyperplasia in the hilar and extrahepatic portal vein suggestive of pre-existing abnormalities. One patient developed progressive portal VT leading to graft failure and a second LT. Post-transplant VT in all 6 patients is ongoing requiring multiple thrombectomies, angioplasties, anti-coagulation, and increased hospital stay. One patient with limited records (and no mention of VT) has died of disease, while the rest are alive.
Conclusion: Pediatric LT for A1AT is uncommon. Majority (75%) of children in our series showed post-transplant VT resulting in increased morbidity and hospital stay with rare loss of allograft; consistent with recent adult reports. Careful pathologic sampling and evaluation of the portal and hepatic veins is necessary at the time of LT to document pre-existing abnormalities, if any. A1AT deficiency should be considered a serious risk factor for venous thrombosis and warrants optimal risk management and careful clinical follow-up.

25

ALK-positive histiocytosis – Clinical and pathologic spectrum: a report from a single institution

A Glembocki, B Ngan, R Chami; Hospital for Sick Children, Toronto, Ontario

Background: ALK-positive histiocytosis is a rare subtype of histiocytic tumour first described as an infantile multisystemic disease with liver and hematopoietic involvement. However, the spectrum of ALK-positive histiocytosis has recently been broadened to include localized/single-system disease and different age groups. Herein, we describe four pediatric cases of ALK-positive histiocytosis showing variable clinicopathological and molecular findings.

Methods: Non-Langerhans cell histiocytosis (LCH) diagnosed during the last three years at our institute were reviewed. Clinical information was documented. Morphology and immunophenotype were reviewed. Additional immunohistochemical and/or molecular analyses were performed when deemed appropriate. Four cases meeting criteria for ALK-positive histiocytosis were identified and included in the study.

Results: All patients showed a localized disease without neurologic involvement; one with a single lung lesion, two patients with a solitary scalp lesion, and one patient with a subglottic mass. Ages (1 female & 3 males) ranged from 2 to 12 years old. The morphology varied and included classic xanthogranuloma features with lipidized histiocytes and some Touton giant cells (1 scalp lesion), dense cellular appearance with plump ovoid to spindle cells with fascicular and/or storiform growth patterns admixed with lymphocytic infiltrate (lung lesion and 2nd scalp lesion), to sheets of mainly epithelioid histiocyte-like cells (subglottic lesion). Nuclear features varied and included ovoid vesicular nuclei with regular nuclear contour, to ovoid nuclei with mild fold or indentation of its contour. Ki-67 proliferation indexes were low to moderate. No necrosis was present. The lesional cells were immunoreactive to CD163 and CD68 (diffuse), and ALK (focal to patchy, weak to moderate cytoplasmic staining), and negative for S100. Three cases showed KIF5B/ALK fusion, and the 4th case showed EML4/ALK fusion (all detected by TruSight RNA-Seq panel). All cases were treated by surgical resection only. Tumor's sizes ranged from 1.0 cm to 6.0 cm. Two cases were well-defined and unencapsulated and were completely excised, and the others had an infiltrative-type border with neoplastic cells extending to the resection margins.

Conclusion: ALK-positive histiocytosis is a distinct entity with a variable clinicopathologic spectrum. It may present as multi- or single-system disease. Our patients had localized disease, and the lesions were treated by surgical resection only. Three cases were recently diagnosed, and one case had no recurrence after 4 years. An integrated histological, immunohistochemical and molecular approach with ALK status evaluation is recommended, particularly in cases of non-LCH, as this may affect disease classification and therapeutic decision making.

26

Pediatric Endometriosis - An Institutional Study

L Biederman, A Shenoy, S Chen; Nationwide Children's Hospital, Columbus, Ohio

Background: Endometriosis is a common gynecologic cause of chronic pelvic pain in female pediatric patients (≤21y). The diagnosis is typically made on biopsy which aids in therapeutic decision making. By definition, a diagnostic biopsy has two of the following three components: endometrial glands, stroma, and/or hemorrhage/hemosiderin-laden macrophages. We performed a retrospective review evaluating our institutional experience with biopsy diagnosis of endometriosis.

Methods: We reviewed the Pathology files from a pediatric tertiary care hospital with an adolescent gynecologic practice between 2015-2021 for female patients who were biopsied for evaluation of endometriosis. Histologic slides were reviewed along with clinical data including imaging, medication history, intraoperative findings, and follow up.

Results: We identified 140 cases (age range: 10-21y; median 17y) in which biopsies ranging from 1-5 sites, including anterior and posterior cul de sac as well uterosacral ligaments, were performed to evaluate for endometriosis. Of these, 69% contained diagnostic findings, 19% were negative and 12% were inconclusive (containing only one of the three required components definitively). Diagnostic biopsies had an average size of 7mm (range: 2-20mm; median 8mm), negative 4.7mm (range: 1-11mm; median 4mm), and inconclusive 6mm (range: 1-15mm; median 6mm). Levels were performed in at least one biopsy site in 94% of diagnostic biopsies, 93% of negative biopsies, and 100% of inconclusive biopsies. Additional sections in at least one biopsy site demonstrated a subsequent diagnostic feature in 63% of the diagnostic cases. Calcifications were associated with 30% of diagnostic biopsies, 23% in negative biopsies, and 41% in inconclusive biopsies.

Conclusion: In this study, a vast majority (69%) of patients biopsies received histologic confirmation of suspected endometriosis. On average, diagnostic biopsies were larger than negative biopsies. Our study demonstrates that biopsy size positively correlates with diagnostic findings, and, in general, biopsies >5mm more likely to be diagnostic. In addition, we demonstrate the usefulness of levels (additional sections) in biopsy specimens and the lack of specificity of calcifications in the biopsy specimens.

27

Activated CD8+ T cell hepatitis phenotype in Indeterminate Pediatric Acute Liver failure: An institutional experience

M Smith[1], B Fung[2], P Kreiger[3], S Mangray[2], C Gariepy[2], C Potter[2], A Weymann[2], R Abraham[2], A Shenoy[2];
[1]Nationwide Children's Hospital, Columbus, Ohio; [2]Nationwide Children's Hospital and The Ohio State University, Columbus, Ohio; [3]Children's Hospital of Philadelphia/University of Pennsylvania, Philadelphia, Pennsylvania

Background: In some patients with pediatric liver failure, the etiology is unidentified, despite thorough diagnostic evaluation. A multicenter study from the Pediatric Acute Liver Failure study group has recently characterized an "Activated CD8+ T cell hepatitis" phenotype in patients with Indeterminate Pediatric Acute Liver Failure (IND-PALF). We report our institutional experience with the diagnosis of activated CD8+ T cell hepatitis in suspected IND-PALF.

Methods: At our institution, in the past 2 years, three patients have been histologically confirmed to have an activated CD8+ T cell hepatitis phenotype. Additional extensive immunophenotyping showed significant immune dysregulation. Medical records were reviewed for demographics, clinical presentation, and serologic findings. Salient pathologic findings are summarized.

Results: All three patients (7//M, 4/F and 8//M) presented with jaundice, transaminase elevation and fatigue. Clinical work-up was negative for infections and non-diagnostic for autoimmune hepatitis [all had positive ANA screen (1:40 – 1:80) and negative ASMA and ALKM-1 antibodies]. Peak INR elevation was pronounced in one patient (>9); mild in two others (1.5 - 1.6). All patients variably met some criteria (2 – 4) for hemophagocytic lymphohistiocytosis (HLH), such as fever, splenomegaly, low fibrinogen and pancytopenia. Elevated serum soluble IL-2R (range: 3122 – 8956 units/ml) was consistently noted. However, hemophagocytosis was absent on liver histology and bone marrow evaluation. Immunophenotyping revealed significant T cell activation with expansion of senescent and exhausted T cells. Liver biopsy demonstrated severely active hepatitis with both portal and lobular inflammation and multifocal hepatocyte necrosis. A diagnosis of activated T cell hepatitis phenotype was confirmed by the increased CD8, CD103 lymphocytes and perforin-positive cells in portal and lobular areas. The CD8+CD103+ T cells are consistent with a tissue-resident memory (TRM) T cell phenotype. Following immunosuppressive therapy, marked improvement in transaminases was observed with histologic improvement on two follow-up biopsies. Subsequently, one patient underwent bone marrow transplantation for aplastic anemia and a second patient is being monitored for evolving aplastic anemia. The 3rd patient has had a remarkable recovery. Currently, none of the patients are listed for transplantation (follow up: 3 months – 2.5 years).

Conclusion: IND-PALF can present with laboratory features suggestive of HLH. An immunohistochemical panel assists in the diagnosis of activated CD8+ T cell hepatitis with expansion of CD103+ TRM T cells in established and impending IND-PALF. Immunological evaluation was crucial in timely selection of immunosuppression and identifying biomarkers for prognostic monitoring.

28

Acute interstitial nephritis in the pediatric population: A review of etiologic associations, histologic findings and clinical outcome

L Biederman, M Conces, A Shenoy; Nationwide Children's Hospital, Columbus, Ohio

Background: Acute interstitial nephritis (AIN) is an infrequent cause of acute kidney injury in the pediatric population. Etiologic associations are broad including medications, autoimmune disorders, and infections. This retrospective review attempts to characterize AIN in the pediatric population, delineate etiologic factors, histologic features, and clinical outcome.

Methods: Institutional pathology reports were queried for a diagnosis of AIN between 1/2010 to 10/2021. Archived slides and reports were reviewed in detail and cases with a concurrent immune complex deposition disease, chronic interstitial nephritis, as well as significant glomerular disease were excluded. Clinical records were reviewed for demographic data, renal function laboratory tests, suspected etiology, and follow-up information.

Results: Twenty-four patients were identified, thirteen males and eleven females whose ages ranged from 5 – 20 years (Median:13 years). Eight cases (37.5%) were characterized as tubulointerstitial nephritis and uveitis (TINU), four cases (16.7%) were associated with an autoimmune disease and four cases (16.7%) were likely drug induced. Etiology for eight cases (37.5%) remained unclear . Although all cases of drug induced interstitial nephritis contained eosinophils, as expected, they were not exclusive to drug induced interstitial nephritis and were seen in cases with unknown etiologies and in TINU. A prominent plasma cell infiltrate was seen in both cases of Sjogren's associated interstitial nephritis, one case of unknown etiology, and one case of unspecified systemic autoimmune disease. The pattern of cortical involvement was variable (patchy vs diffuse) across etiologies. The vast majority (n =186, 75%) showed an improved serum creatinine (<1 mg/dL) one year post diagnosis/at last follow-up. Most of the cases (n=4, 66.7%) that did not show improvement of the serum creatinine had chronic parenchymal changes (interstitial fibrosis and tubular atrophy and global glomerulosclerosis) at the time of biopsy. Of the 2 cases that did not, one had granulomas and was suspected sarcoidosis, and the other was a case of TINU with diffuse cortical involvement and early chronic changes of the tubules.

Conclusion: In this pediatric series of AIN, TINU contributed to a large subset of cases with known etiolgies, while autoimmune and drug related AIN was less frequent. Etiology of a subset of cases remained unrecognized. Eosinophilic infiltrate was variably noted both in drug and non-drug associated AIN. On follow up, majority of the cases demonstrated recovery of renal function. In the subset with persistent renal dysfunction, several cases demonstrated histologic features of chronic parenchymal changes/injury.

29

Current Utilization of Electron Microscopy in the Pediatric Pathology Setting: A Survey by the SPP Practice Committee

M Warren[1], R Reed[2], V Prasad[3], V Rajaram[4], D Roberts[5], S Besmer[6], L Darrisaw[7], P Kreiger[8], D Lopez-Terrada[9]; [1]Children's Hospital Los Angeles, Los Angeles, California; [2]Seattle Children's Hospital, Seattle, Washington; [3]Nationwide Children's Hospital, Columbus, Ohio; [4]UT Southwestern/Children's Health, Dallas, Texas; [5]Massachusetts General Hospital, Boston, Massachusetts; [6]Cardinal Glennon Children's Hospital, St. Louis, Missouri; [7]Georgia Bureau of Investigation, Decatur, Georgia; [8]4. Children's Hospital of Philadelphia, Philadelphia, Pennsylvania; [9]Texas Children's Hospital, Houston, Texas

Background: It is perceived that diagnostic indications for electron microscopy (EM) have declined and on-site EM services have been discontinued; however, the details of the practice are unknown. The purpose of this survey is to investigate the status of current EM practice in pediatric pathology.
Methods: We administered a16-question survey regarding EM services. The participants were 113 SPP members practicing in 74 different hospitals, including 36 academic tertiary hospitals (ATH), 32 free-standing children's hospitals (FCH), and 6 community-based hospitals (CH).
Results: 50% and 27.8% of ATH reported receiving >25,000 and 5,000-15,000 surgical specimens/yr, respectively, while many FCH (62.5%) received 5,000-15,000/yr. Although only 6 CH participated, 2 received >25.000 and others had <1,000 to 15,000/yr. Most ATH and FCH reported 1-5 or 6-10 pediatric pathologists (PP) practicing in their laboratories, while CH reported fewer (<5) PP. 14/36 (38.9%) ATH and 18/32 (56.2%) FCH had pediatric pathology fellowship programs; of these, 17/32 (53.1%) included EM training in their curricula. Many ATH (28/36, 77.8%) and FCH (19/32, 59.4%), but no CH (0/6, 0%) had at least 1 electron microscope (total 47/74, 63.5%); 10 had >1 electron microscopes. 45/74 hospitals (60.8%) processed EM specimens and interpreted EM images in their laboratories. 40/66 (60.6%) hospitals reported having >2 specialized pathologists interpreting EM, while most reported 0-2 EM technologists. Turnaround time for EM sign-out was distributed from 1-2 days to 28 days. Pediatric EM specimen volumes ranged from 0 to >500/year, with a majority of ATH and FCH reporting 50-100 and 100-200 cases/year, respectively. Institutions reporting fewer cases (<50) tended to send the specimens to reference EM laboratories. 17 hospitals that terminated their EM services reported stopping in-house EM services, mostly after 2000, due to low case volume (n=10), high operating costs (n=8), lack of EM technologists (n=8), lack of pathologists specialized in EM (n=5), and better alternative ancillary testing (n=3). Diagnostic EM was most often performed on kidney, liver, cilia, heart, and muscle, and fewer institutions used EM for lung, tumor, skin, GI, autopsy, platelet, nerve, BAL, and microbiology specimens. FCH tended to perform EM on a wider range of diagnostic specimens than ATH and CH.
Conclusion: Although some institutions are facing challenges maintaining their EM services, the survey revealed >60% of the participating institutions owned electron microscope(s) and processed/interpreted their EM cases, mostly kidney, liver, and cilia specimens. 51.3% of pediatric pathology fellowship programs included EM training in their curricula. These results indicate, despite difficulties, EM is still in active use by pediatric pathologists.

30

Histiocyte Rich Rhabdomyoblastic Tumor: Case Report and Review of the Literature

J Gulliver[1], M Elhodaky[2], A Richardson[1], N Arva[1], N Wadhwani[1]; [1]Lurie Children's Hospital, Chicago, Illinois; [2]Northwestern University Feinberg School of Medicine, Chicago, Illinois

Background: Tumors with rhabdomyoblastic differentiation represent a diverse spectrum of entities from benign to malignant. Categorizing these tumors is important for determining appropriate clinical management, surgical approach, and if neoadjuvant or adjuvant therapy is warranted. We report a case of a rare histiocyte rich rhabdomyoblastic tumor in a pediatric patient.

Methods: We reviewed available clinical, radiologic, pathologic, immunohistochemical, and molecular data as well as cases currently described in the literature.

Results: A 5 year old male presented with a painless lump present for at least a month. He was found to have a right thigh mass. Ultrasound showed a heterogenous mass in the right distal vastus medialis with internal vascularity. Subsequent MRI showed a lobulated T2 hyperintense and T1 hypointense 4.6 cm mass in the right distal vastus medialis with internal nodular hypoenhancement and peripheral hyperenhancement. The mass mostly did not invade the fascia. A biopsy of the mass showed a proliferation of spindled and epithelioid cells with dense, eosinophilic cytoplasm with interspersed macrophages and giant cells with histiocytic differentiation and Touton-like morphology. The patient went on to have a resection. The resection specimen showed the same morphology as the biopsy. The lesional cells were diffusely positive for Desmin, CD163, and Factor XIIIa. There was limited MyoD1 and Myogenin expression. BAF-47 was retained. CAM5.2, SMA, ERG, CD1a, and EMA were negative. Molecular testing was performed. The lesion was negative for PAX3-FOXO1 and PAX7-FOXO1 gene fusions. DNA analysis identified a variant of clinical significance in KRAS and variant of unknown clinical significance in CHD7. The patient at one month follow up has not had recurrence.

Conclusion: Histiocyte rich rhabdomyoblastic tumor is a rare tumor with uncertain behavior. To our knowledge, this is the youngest aged patient to present with a histiocyte rich rhabdomyoblastic tumor. Most cases of histiocyte rich rhabdomyoblastic tumor occur in males, similar to our case, but patients are typically young to middle aged. The tumors have a predilection for the extremities but have been described in other sites. This entity is a potential diagnostic pitfall for malignant rhabdomyoblastic tumors. Recognition is important as this could potentially be a tumor that may not necessarily need aggressive treatments such as radiation or chemotherapy which carry associated toxicities and have long term consequences both for pediatric and adult patients.

31

First Report of Comprehensive Genomic Profile of Pre-Sacral Medulloepithelioma

M Smith[1], S Chen[2], K Schieffer[2], M Ranalli[2], J Aldrink[2], D Boue[2]; [1]Nationwide Children's Hospital, Columbus, Ohio; [2]Nationwide Children's Hospital and The Ohio State University, Columbus, Ohio

Background: Medulloepithelioma is a malignant neuroepithelial tumor in the Embryonal Tumor with Multilayered Rosettes (ETMR) family of CNS tumors. Medulloepitheliomas are rare, highly aggressive tumors with poor prognosis, most commonly seen in the CNS of young children. The neoplasms are typically intracranial. CNS tumors are most often C19MC altered (90%). Reported alterations include amplification and fusions at 19q13.42. In contrast, extracranial (peripheral) medulloepitheliomas are exceedingly rare with few case reports and have different genetic profiles despite similar morphology. Rare extracranial medulloepitheliomas have been reported mostly in the intraocular/ciliary body, less so in the pre-sacral region.

Methods: We evaluated a 1-year-old female who presented with presacral swelling initially suspected to be an abscess or congenital anomaly. MRI revealed a large, solid homogeneous mass in the sacrococcygeal region with a differential of sacrococcygeal teratoma (no cystic, fatty, or bony/cartilaginous components), neuroblastoma, or rhabdomyosarcoma. She was also found to have multiple liver lesions and enlarged regional lymph nodes and nerve roots.

Results: Initial histology revealed predominantly medulloepithelioma with scattered foci of small round blue cell tumor. Immunohistochemical evaluation revealed a staining pattern consistent with medulloepithelioma. PAS stain revealed both internal and external limiting membranes. There was diffuse-patchy pancytokeratin, patchy strong LIN28a, focal synaptophysin and neurofilament, and very focal S100, GFAP, and Olig-2 immuno-reactivity. Ki-67 index was >80% diffusely. Specific markers for neuroblastoma and rhabdomyosarcoma were negative. The patient was consented for comprehensive genomic studies. Patient blood was negative for disease-associated germline variants. The tumor harbored a somatic SETBP1 variant, p.Asp868Asn, and copy number gains in chromosomes 2, 3, 8, 12, 17, and 20. DNA methylation studies (using DKFZ CNS tumor classifier v12.3) revealed consistency with ETMR, C19MC non-amplified, with a score of 0.93663.

Conclusion: We present the first report of comprehensive clinicopathologic, radiologic, and genomic evaluation of pre-sacral medulloepithelioma. The tumor was found to harbor a SETBP1 somatic variant, enriched in the setting of hematologic malignancy, with rare documentation in CNS tumors. The DNA methylation profile was consistent with intracranial (CNS) ETMR, C19MC non-amplified. At the time of this report, the patient had interval response to chemotherapy including shrinkage of the primary and metastatic lesions. Subsequent resection showed partial therapy response. We are also attempting to perform comprehensive genomic profiling on an intraocular medulloepithelioma from our case files.

32

Acute Myeloid Leukemia (AML) with RAM-Immunophenotype and CBFA2T3-GLIS2 Fusion Transcript; Rare Entities of Pediatric AML

J Gulliver, S Gong, K Yap, A Richardson; Lurie Children's Hospital, Chicago, Illinois

Background: The RAM-immunophenotype acute myeloid leukemia (AML) represents a rare subtype of pediatric AML, characterized by bright CD56, dim/negative CD45, dim/negative CD38 and negative HLA-DR expression. This entity is clinically associated with an extremely poor prognosis. In a small study of 16 patients with AML with RAM phenotype, 63% were reported to have CBFA2T3-GLIS2 fusion transcript by Pardo et al. in 2020. We sought to further characterize this rare entity, based on WHO and FAB classification, and molecular findings as identified by next-generation sequencing and clinical outcome.

Methods: Within our archives, we identified five patients (4 patients, age 1-3 and 1 patient age 14 at the time of diagnosis) with AML with RAM-immunophenotype. We reviewed available clinical, histologic, immunohistochemical, flow cytometry, and molecular data. Next generation sequencing (NGS) was performed on RNA and DNA isolated from fresh bone marrow aspirate.

Results: While all 5 patients were diagnosed with AML, 3 patients had non-Down syndrome acute megakaryoblastic leukemia, French-American-British (FAB) M7 and 2 patients had acute myeloid leukemia with minimal differentiation, FAB M0. CSF of all 5 patients was negative. NGS detected CBFA2T3-GLIS2 fusion transcript, variant of strong clinical significance in 3 patients (60%, 2 patients diagnosed with AML-FAB classification M7, 1 patient diagnosed with AML-FAB M0). Interestingly, 2 patients of which both had AML-FAB M0 were found to have variants of potential clinical significance (1 patient had only pathogenic variant in IKZF1 while 1 patient had pathogenic mutation in JAK2 in addition to CBFA2T3-GLIS2). All five patients underwent induction chemotherapy, often undergoing a second cycle of chemotherapy. The patients were followed by flow cytometry, presence of CBFA2T3-GLIS2 fusion transcripts, and cytogenetic testing. All patients underwent stem cell transplant. 2 patients (1 patient with AML-FAB M7 without CBFA2T3-GLIS2 fusion, 1 patient with AML-FAB M0 and CBFA2T3-GLIS2 fusion and JAK2 mutation) relapsed and died two years after stem cell transplant.

Conclusion: CBFA2T3-GLIS2 fusion is a result of cryptic inversion of chromosome 16 [inv(16)(p13.3q24.3)], thus is not detected by conventional cytogenetic testing. Although CBFA2T3-GLIS2 fusion transcript is present in almost 20% of pediatric non-Down syndrome acute megakaryoblastic leukemia, it is not exclusively restricted to the AML-FAB M7 subgroup and is seen in approximately 60% of patients with AML with RAM-immunophenotype. Importantly, RAM-immunophenotype and CBFA2T3-GLIS2 fusion are independent risk factors; both are associated with younger age, high rate of induction failure, and poor outcome. They require aggressive treatment to improve outcome and are a rare form of pediatric AML.

33

Intracranial mesenchymal tumor with PLAG1 gene fusion (PLAGoma)

S Sethi, J Park, D Rakheja, R Collins; UT Southwestern Medical Center, Dallas, Texas

Background: A 9-month-old male with abnormal head movement and dysconjugate gaze was found to have right superficial cerebellar masses with obstructive hydrocephalus. At initial surgery, four nodular masses were excised ranging in size from 0.8-4.1 cm. There was clinical recurrence within 3 months and the recurrent tumors were also excised.

Methods: The pathologic specimens were examined by routine histology and electron microscopy (EM) and interrogated by immunohistochemistry, karyotyping, fluorescence in situ hybridization, and next generation sequencing (NGS) for gene fusions.

Results: Grossly, the masses were nodular and circumscribed with homogenous pale white, vaguely lobular, rubbery cut surfaces. Low power showed a cellular neoplasm composed of wavy, spindle cells arranged in short fascicles, with a vaguely nodular architecture and areas of moderate cellularity interspersed with edematous foci. The nuclei were oval to elongate with vesicular chromatin and inconspicuous to punctate nucleoli. A few cells with large hyperchromatic nuclei were present scattered, and rare multinucleated cells were noted. Mitoses were rare (<1/10 HPF) in the initial excisions; however, in the recurrence, mitoses were up to 11/10 HPF. Focal tumor necrosis was also present in the recurrent tumor. The tumor cells showed diffuse strong nuclear staining for PLAG1, diffuse cytoplasmic staining for BCL2, and patchy membranous and cytoplasmic staining for GLUT1. They showed focal weak staining for desmin, TLE-1, CD34, SST-2A, and NKI-C3; were negative for SMA, SOX10, EMA, MUC-4, STAT6, myogenin, MyoD1, GFAP, synaptophysin, and S100; and showed retained nuclear staining for H3K27me3. EM revealed the tumor cells to have sparse organelles including mitochondria and rough endoplasmic reticulin, and occasional lipid droplets. Fluorescence in situ hybridization for FUS and EWSR1 gene rearrangements were negative. Targeted gene fusion analysis by NGS identified a fusion between PCMTD1 (exon 1) and PLAG1 (exon 2). Conventional chromosomal analysis showed a complex karyotype (55,XY,+2,+del (5)(p13p15),+7,+11,+12,+18,+mar,+mar).

Conclusion: PLAG1 is a transcription factor known to be rearranged in pleomorphic adenomas and lipoblastomas. PCMTD1::PLAG1 fusion has only rarely been reported: in a fibroblastic lipoblastoma in the neck of a 4-year-old female and in a spindle cell tumor in a finger of a 1-year-old male. We describe here for the first time PCMTD1::PLAG1 fusion in an infantile intracranial tumor. Although previously described PLAGomas demonstrated a benign clinical course, the tumor described here initially appeared low grade but had a concerning complex karyotype and evolved to higher grade within 3 months.

34

Focal Nodular Hyperplasia in the Pediatric Population: single center experience

I Gonzalez, P Russo; Children's Hospital of Philadelphia, Philadelphia, Pennsylvania

Background: Focal nodular hyperplasia (FNH) is a benign, non-neoplastic process, thought to result from hepatocyte hyperplasia due to an altered blood flow. In the pediatric population FNH are rare with only small series reported, hence their detailed clinicopathologic characteristics remain largely unknown. In this study we present the largest cohort, to our knowledge, of FNH in pediatric patients and their clinicopathologic features.

Methods: A search was made for cases with a diagnosis of FNH from 1995-2021. All cases and background liver materials (if available) were reviewed blinded to the clinical information.

Results: 24 cases were included in the study, presenting with a median age of 10.2 (0.1 to 17.8) years; of those 8 (33%), 6 (25%) and 10 (42%) patients presented in <6, 6–12 and 12–18 years of age, respectively. Almost an equal gender distribution was seen with 13 (54%) cases presenting in boys but in patients <6 years 75% of the cases presented in boys. 13 (54%) of the cases were diagnosed on biopsies. In 10 (42%) patients multiple FNH were identified ranging from 3 to 6 lesions in 5 cases and in the other 5 these were innumerable. The median size was 3.9 (1.5–11.7) cm. The following histologic features were identified: central scar in 14 (58%), fibrous septa in 23 (96%), dystrophic vessels in 10 (42%), ductular reaction in 23 (96%), cholate stasis in 9 (38%), inflammation in 3 (13%), sinusoidal dilatation in 3 (13%), telangiectasia in 10 (42%), unpaired arteries in 18 (75%), pseudoacinar formation in 3 (13%), and steatosis in 5 (21%) cases. In one case multifocal extramedullary hematopoiesis and in another one non-necrotizing granulomas were identified within the lesion. An underlying liver disease was seen in 3 cases (hepatoportal sclerosis, congenital hepatic fibrosis and biliary atresia) and in 4 cases an underlying liver neoplasm was seen (3 hepatocellular adenomas and 1 angiosarcoma). In 6/18 patients (33%) whose medical histories were available, a history of an underlying malignancy was noted (neuroblastoma, 3 cases; atypical rhabdoid tumor and osteosarcoma, 1 case; Wilms tumor and Ewing sarcoma, 1 case; Hodgkin lymphoma, 1 case); 5 of them received chemoradiation therapy and a stem cell transplant. In 3 patients a vascular abnormality was seen. Two patients had a uniparental disomy of chromosome 11. The median follow-up time, available in 19 cases, was 40 (1 to 154) months.

Conclusion: We present the largest cohort of FNH in our pediatric population and their clinicopathologic characterization. A common association is the presence of an underlying malignancy treated with chemoradiation and stem cell transplant. Understanding of these characteristics will assist in the diagnostic workup of these rare lesions which often pose a diagnostic challenge.

35

Congenital hepatoblastoma in a patient with Costello syndrome: coincidence or association?

M Takeda, M Warren, F Navid, J Ji, J Biegel, S Zhou; Children's Hospital of Los Angeles, Los Angeles, California

Background: Congenital hepatoblastoma is rare with less than 50 cases reported in the literature. Association between hepatoblastoma and hemihypertrophy, Beckwith–Wiedemann syndrome, and low birthweight has been well documented. However, to our knowledge, hepatoblastoma has not been previously reported in patients with Costello syndrome, which is caused by heterozygous pathogenic variants in the HRAS gene. Herein, we describe a patient with Costello syndrome who presented with congenital hepatoblastoma.

Methods: Patient clinical information was retrieved from the electric medical record. A singleton-exome sequencing was performed on the peripheral blood sample using the Agilent SureSelect Human All Exon V6 kit. OncoKids® next-generation sequencing (NGS) cancer panel and chromosome microarray (CMA) were performed on the liver tumor (Affymetix OncoScan FFPE Assay).

Results: A newborn, ex-29 week premature male, whose prenatal course was complicated by polyhydramnios and enlarged fetal liver, was found to have a 4.5 cm liver mass on imaging and elevated AFP (352,000 ng/mL). Wedge biopsy of the mass showed a heterogenous malignancy with two distinct epithelial components: one with pleomorphic nuclei and scant eosinophilic cytoplasm (embryonal); and the other with small, centrally located nuclei and pale abundant cytoplasm (fetal). On immunohistochemistry, tumor cells showed positivity for glypican 3, patchy positivity for SALL4, and focal cytoplasmic positivity for beta-catenin. The immunohistological features were consistent with the diagnosis of congenital hepatoblastoma, epithelial type, with fetal and embryonal components. NGS panel performed on the tumor demonstrated a mutation in CTNNB1 p.Ser45Phe and CMA showed a gain of chromosome 2. These molecular findings supported the pathologic diagnosis of hepatoblastoma. Interestingly, NGS of the tumor and constitutional exome sequencing also demonstrated HRAS p.Gly12Ser, a well-established pathogenic variant associated with Costello syndrome. The additional clinical features noted since his birth including atrial tachycardia, arthrogryposis-like hand anomaly, camptodactyly, and abnormality of the thorax and pinna, with the presence of a germline HRAS pathogenic variant were consistent with the diagnosis of Costello syndrome. Though the patient received 4 cycles of cisplatin-based chemotherapy for his tumor, his clinical course was complicated by respiratory failure, multiple infections, and expired at 6 months of age.

Conclusion: The typical tumors seen in patients with Costello syndrome include rhabdomyosarcoma, neuroblastoma, and transitional cell carcinoma of the bladder. This is the first case of congenital hepatoblastoma in a patient with Costello syndrome, raising a possible association between hepatoblastoma and Costello syndrome.

36

Hepatocellular Malignant Neoplasm, Not Otherwise Specified (HCN-NOS) in a Two-Year-Old Male with Early Cirrhosis and Multiple Dysplastic Nodules

C Le Phong, L Mascarenhas, M Warren, R Schmidt, R Kohli, Y Genyk, S Zhou; Children's Hospital of Los Angeles, Los Angeles, California

Background: Hepatocellular malignant neoplasm, not otherwise specified (HCN-NOS) is a provisional entity with histologic features of neither typical hepatoblastoma (HB) nor hepatocellular carcinoma (HCC). It is rare (< 20 cases reported) and usually seen in children ages 4-15 years old in a background of normal liver. We present here the first HCN-NOS case arising in the background of cirrhosis in a child <4 years of age.

Methods: Clinicopathological features were retrieved from the electronic medical record. OncoKids® NGS panel and chromosome microarray (CMA) were performed on two different tumor nodules.

Results: A 2-year-old, ex-28-week premature male with a complicated medical history including parenteral nutrition for 6-8 months, presented with early cirrhosis, elevated serum AFP (800 ng/mL), and multiple liver nodules on imaging. An outside liver biopsy favored a malignant well-differentiated hepatocellular neoplasm. A deceased donor segmental transplant was performed prior to chemotherapy. The liver explant revealed four grossly well-circumscribed, solid tan to yellow tumors, three in the right lobe (up to 3.5, 1.0, and 0.5 cm) and one in the left lobe (up to 0.5 cm). Histologically, the largest tumor shows a heterogeneous proliferation resembling HB fetal, embryonal, and small cell undifferentiated components, and HCC. Extramedullary hematopoiesis, increased mitosis, and lymphovascular invasion were present. The second largest tumor shows near complete necrosis. The two smaller tumors show overlapping histology between HB and HCC. The background liver shows early cirrhosis and multiple dysplastic nodules. Glypican 3 staining was positive in all tumors (mixed patterns); cytoplasmic positive in the dysplastic nodules, and negative in uninvolved liver. SALL4 was focally positive in the largest tumor; and negative in the other parts. Beta-catenin was positive in all tumors (mixed patterns) and membranous staining in the other parts. OncoKids® revealed a pathologic variant in CTNNB1 (c.100G>A (p.Gly34Arg) in the largest tumor; and a different pathologic variant in CTNNB1 (c.95A>G (p.Asp32Gly) with somatic mutations of unknown significance in the WT1 and DDX3X genes in one of the smaller tumors. Both tumors demonstrated the same copy number alteration (gain of 1q) by CMA. The overall histology, immunostaining and molecular findings supported the final diagnosis.

Conclusion: It is important to consider HCN-NOS beyond HB and HCC in atypical pediatric and adolescent cases as liver transplantation is a proper treatment option for it. This is also the first report of liver malignancy harboring two distinct CTNNB1 mutations. The molecular findings in this case may shed light on the sequence of acquisition of mutations that occur for these tumors.

37

Inflammatory Orbital Pseudotumors in Children: A Series of Three Cases

C Le Phong, M Takeda, M Warren, S Zhou, N Shillingford, B Pawel, L Wang; Children's Hospital of Los Angeles, Los Angeles, California

Background: Fibrous inflammatory lesions of the orbit may present as masses prompting a pathologic workup. The histologic diagnosis is often non-specific and descriptive. Clinical correlation leads to the clinicopathologic differential diagnosis including idiopathic sclerosing orbital inflammation (ISOI) and autoimmune disorders such as IgG4-related disease (IgG4-RD), sarcoidosis and ANCA-associated vasculitis (AAV). Identification of the type of inflammatory infiltrate, the presence of granulomas, and/or vasculitis may be helpful. However, the histologic findings are not always clearcut and are diagnostically challenging. We present a series of three cases of fibrous inflammatory orbital lesions with varying clinical diagnoses based on the integration of the clinical features, laboratory values, and pathologic findings.

Methods: Case 1: A previously healthy 12-year-old girl presented with erythema/swelling of the right eyelid for 3 months. Biopsy showed a lymphoplasmacytic/histiocytic inflammatory infiltrate in a fibrous background. By IHC, the IgG4/IgG ratio was increased. Rheumatologic workup showed elevated p-ANCA and ANA titers. The diagnosis of ANCA-positive, IgG4-RD was made. The patient was treated with steroids and methotrexate. Her disease has remained stable without further therapy for 5 years. Case 2: A 7-year-old girl with history of sensorineural hearing loss presented with left eye swelling and proptosis for 4 months. Biopsy showed dense collagenous lesion with lymphoplasmacytic/histiocytic/eosinophilic infiltrates, suggestive of ISOI. IgG4 IHC was not performed due to sparse plasma cells. Rheumatologic workup revealed elevated p-ANCA and serum IgG4. The diagnosis of AAV was made. A biopsy confirmed renal involvement. She was treated with rituximab, steroids, and mycophenolate. Her disease remains well-controlled after 12 months.

Results: Case 3: An 11-year-old girl with history of being small for age (<5% percentile) presented with elevated ESR and p-ANCA, and hematuria/proteinuria concerning for AAV. A right orbital mass with sinus thickening was discovered. Biopsies at both sites showed dense fibrosis with neutrophilic infiltrates and focal vasculitis. IgG4-RD was ruled out by IHC. A presumptive diagnosis of AAV was made. She is currently on steroid treatment and is doing well after 1 month.

Conclusion: These cases illustrate the overlapping clinical and pathological features amongst these inflammatory orbital entities. It is important to distinguish AAV and IgG4-RD from ISOI as the treatment regimens and intensities vary. Additionally, IgG4-RD is a multiorgan disease and carries a risk of lymphoma, warranting more vigilant surveillance. The definitive diagnosis often requires the integration of all clinical, pathologic, and laboratory data.

38

Angiomatoid Fibrous Histiocytoma with Predominant Xanthogranulomatous Morphology Presenting as Large Submandibular Mass: A Diagnostic Pitfall

M Smith[1], S Kahwash[2]; [1]Nationwide Children's Hospital, Columbus, Ohio; [2]Nationwide Children's Hospital and The Ohio State University, Columbus, Ohio

Background: Angiomatoid fibrous histiocytoma (AFH) is a rare soft tissue lesion primarily seen in children and young adults. These lesions have intermediate malignant potential with rare reports of metastases. They most often arise in the subcutaneous tissue of the extremities and present as a painless and slow growing mass. Clinical and radiologic findings are nonspecific. AFH can display an array of clinical, radiologic, and pathologic features leading to misdiagnoses. The classic histologic example of an AFH shows a fibrous pseudocapsule with a dense peripheral lymphoplasmacytic cuff, pseudoangiomatous spaces lined by tumor cells (no true endothelial lining), and cytologically bland ovoid to spindled cells in a variety of patterns.

Methods: We evaluated a soft tissue mass from the submandibular region of a 12-year-old male. The child had clinical history of a painless, slowly enlarging mass present for 9 months. It had been evaluated multiple times with reassurance provided until it began enlarging more rapidly. An ultrasound revealed a heterogeneous and hyperemic mass with a broad differential diagnosis. He was referred for surgical resection. He reported occasional night sweats and was found to have anemia during perioperative evaluation.

Results: Initial resection showed lymph nodes with reactive follicular hyperplasia surrounding fibrous and lesional tissue. The lesion was composed of sheets of histiocytic cells admixed with variable infiltrates of eosinophils, neutrophils, lymphocytes and plasma cells, all surrounded by areas of thick fibrous tissue and lymphoplasmacytic infiltrates. Lesional cells showed a broad range of morphologic variability, from histiocytic to fibrohistiocytic with multiple of foci of lipid-rich cells. Focal areas showed multinucleated Touton-type giant cells. The diagnosis was initially rendered as atypical xanthogranulomatous histiocytic lesion, and the case was sent for molecular characterization. The molecular testing revealed an EWSR1-ATF fusion, and the amended diagnosis was angiomatoid fibrous histiocytoma with EWSR1-ATF fusion.

Conclusion: Angiomatoid fibrous histiocytomas can have a spectrum of clinical and morphologic features, which can create potential diagnostic pitfalls. In this case, the specimen was received fragmented, which altered the overall architecture of the lesion. The abundance of xanthomatous cells initially raised a differential diagnosis of juvenile xanthogranuloma and other xanthomatous lesions. Finally, the pseudoangiomatous features were not readily apparent. These confounding factors highlight the importance of molecular testing panels.

39

The criteria for microscopic examination of tonsils in pediatric population

H Tang[1], B Su[2], R Morotti[3], H Wu[3]; [1]Yale New Haven Hospital, New Haven, Connecticut; [2]Acton Boxborough Regional High School, Acton, Massachusetts; [3]Yale School of Medicine, New Haven, Connecticut

Background: Most pediatric bilateral tonsillectomy is performed for symptomatic relief in tonsillar hypertrophy and obstructive sleep apnea. Clinically actionable pathologic findings (CAPF) in pediatric tonsils are extremely rare. Different triaging protocols tailored towards individual otolaryngologists creates workflow difficulties for pathology laboratories. We examined the preanalytical variables that had the highest predictive value for CAPF.

Methods: This study was approved by the institutional review board. Pediatric (age 1-21) bilateral tonsillectomy with clinical request for lymphoma workup from 2008 to 2021 was identified, with transplant patients excluded. The submitted clinical history and the gross measurements were tabulated. Receiver operating characteristic (ROC) and area under the curve (AUC) were compared for the search of the best predictor for CAPF.

Results: 43 patients aged 2-21 years were included (median 12). Fives had CAPF: 3 Burkitt lymphoma, 1 infectious mononucleosis (IM), and 1 necrotizing lymphadenitis. The rest of the patients had a diagnosis of reactive hyperplasia on both histologic examination and flow cytometry analysis. There was no statistically significant age difference between the CAPF and non-CAPF groups ($p = 0.98$). The submitted clinical history was tonsillar hypertrophy for all, with asymmetry mentioned in 14. Clinically observed asymmetry had no correlation with measured asymmetry ($p > 0.05$). The mean and 95% confidence interval (CI) of the length and width of the tonsils were 3.1 cm (2.9-3.3 cm) and 2.2 cm (2.1-2.4 cm), respectively. The measurements of the diseased tonsils were significantly larger than those of the reactive ones ($p < 0.05$). When the length and width were used to predict CAPF, the AUC were 0.89 and 0.90, respectively. The patient with IM had emergent tonsillectomy for breathing difficulty and had bilateral disease. All other 4 patients had unilateral CAPF, with length at least 1.0 cm larger in the diseased tonsil than the uninvolved tonsil. The mean and 95% CI of the bilateral length difference (LD) and width difference (WD) were 0.4 cm (0.3-0.6 cm) and 0.46 (0.3-0.6 cm), respectively. When the LD and WD were used to predict CAPF, the AUCs were 0.92 and 0.83, respectively. When the IM patient was excluded for analysis, the AUCs were 0.98 and 0.94 for the LD and WD, respectively. Using a bilateral LD more than 1.0 cm would have a true positive rate of 1.0, false positive rate of 0.078, with false negative rate at 0.

Conclusion: Based on AUC, LD is the best criterion in selecting tonsillectomy for histologic examination. Even though length alone is not the best predictor, enlargement that compresses the airway should be another indication for pathologic examination.

40

Inflammatory cloacogenic polyp of the created vagina in repaired cloacal anomaly.

P Rungsiprakarn[1], E Doolin[2], T Kolon[2], P Kreiger[2]; [1]Children's Hospital of Philadelphia, Philadelphia, Pennsylvania; [2]Children's Hospital of Philadelphia and University of Pennsylvania, Philadelphia, Pennsylvania

Background: Inflammatory cloacogenic polyp (ICP) is a benign polyp arising from the anorectal transition zone. ICP has been associated with multiple conditions (e.g. rectal prolapse, internal hemorrhoids, Crohn disease) for which mucosal injury has been the purported pathogenic mechanism. Cloacal anomaly is a complex anorectal malformation characterized by a confluence of the rectum, vagina, and urethra exiting the perineum through a single common orifice. Very rare case reports have described ICP in the vagina but not in association with cloacal anomaly. Herein, we report the first case of an ICP occurring in the created vagina of a patient with repaired cloacal anomaly, suggesting a developmental mechanism in this patient.

Methods: A 16-year-old female with a complex past medical history including cloacal anomaly status post reconstruction and bladder augmentation with appendicovesicostomy and bladder neck closure, followed clinically for recurrent urinary tract infections and bladder stones, presented with increased urine mucus and intermittent gross hematuria. The patient underwent cystoscopy and vaginoscopy. Thick mucus was noted in the augmented bladder without concerning lesions or stones. Vaginoscopy showed a hemorrhagic polypoid lesion along the left lateral wall of the created neo-vagina. Biopsies of the vaginal lesion were submitted for pathologic examination. Intraoperative urine culture from the dependent portion of the augment grew Proteus mirabilis sensitive to Bactrim.

Results: Vaginal polyp biopsies consisted of two slightly irregular red-tan pieces of soft tissue each measuring 0.7 x 0.6 x 0.3 cm. Histologic examination of these biopsies revealed benign polypoid fragments of fibrovascular tissue with areas of surface erosion, vascular congestion, dense acute and chronic inflammation, and a mix of surface epithelial types including transitional, simple columnar, intestinal, respiratory, and squamous. No cytologic atypia was seen. The histologic findings were interpreted as an inflammatory cloacogenic polyp of the created vagina.

Conclusion: This case represents the first description of an inflammatory cloacogenic polyp arising in the created vagina of a patient with repaired cloacal anomaly. ICP of the anorectum is thought to arise from anorectal mucosal injury. In this case, we speculate a developmental etiology given this patient's known complex malformation involving both the vagina and anorectum. From a practical perspective, this diagnosis should be entertained in all cloacal anomaly patients with any history of urethrovaginal lesion or bleeding.

41

Rare case of recurrent low-grade glioneuronal tumor featuring EWSR1-PATZ1 gene fusion with myogenic differentiation

K Coxon[1], Y Liu[1], V Paulson[1], E Crotty[2], S Leary[2], A Lee[2], F Perez[2], B Cole[2]; [1]UWMC, Department of Pathology and Laboratory Medicine, Seattle, Washington; [2]Seattle Children's Hospital, Seattle, Washington

Background: An 8-year-old female presented to the emergency department (ED) with a seizure and was discovered to have an enhancing, heterogeneous left frontal lobe mass with cystic and solid components measuring 5.4 x 5.5 x 5.1 cm.

Methods: The patient underwent total surgical resection, and the operative team noted a hard, nodular mass that was discrete from nearby brain tissue. They were able to dissect around the mass and remove it one piece. Immunohistochemical (IHC) stains included S100, CD34, MAP2, GFAP, Desmin, Myogenin, Sox10, Synaptophysin, NeuN, NTRK-pan, EMA, and Ki-67. Molecular profiling included next generation sequencing, methylation profiling, and RNA sequencing. Subsequent surveillance imaging demonstrated a small area of recurrence. The patient was taken back to the operating room for re-resection several months after her first surgery, with additional tissue sent for pathologic evaluation.

Results: H&E stains revealed a moderately cellular neoplasm composed of stellate to spindled cells embedded in a densely collagenous matrix, which was highlighted using trichrome stain. IHC results indicated a low-grade tumor expressing a mixture of glial, neuronal and muscle markers. GFAP only stained 10% of tumor cells. Desmin showed variable patchy positivity. Myogenin and EMA were both negative. MAP2 stained uniformly positive, and S100 was similarly positive in essentially all tumor cells. CD34 was only positive in a subset. The proliferation index was <1%. Molecular profiling using next generation sequencing indicated copy number loss of portions of chromosomes 9 and 22. Methylation profiling showed that the tumor didn't classify with any known group. RNA analysis identified an in-frame fusion for EWSR1PATZ1.

Conclusion: Glioneuronal tumors with EWSR1-PATZ1 gene fusions are exceedingly rare. This case report expands our knowledge of the histologic and clinical spectrum of this tumor. To our knowledge, this is the first reported case with myogenic differentiation. This case also highlights the need for broad molecular profiling in diagnosis of unusual pediatric CNS tumors.

42

Apoprotein L1 Expression in Placenta Specimens by Immunohistochemistry

J Davick[1], J Jarzembowski[2]; [1]University of Iowa, Iowa City, Iowa; [2]Children's Wisconsin, Milwaukee, Wisconsin

Background: Some human gene variants theoretically arise via natural selection by conferring host resistance to infectious diseases but simultaneously cause other disorders. Examples of such theories include sickle cell trait (resistance to malaria) and cystic fibrosis mutations (resistance to tuberculosis and typhoid fever). Apoprotein L1 (APOL1) is a minor apoprotein component of the high-density lipoprotein (HDL). Polymorphisms in the APOL1 gene - two coding variants, termed 'G1' (two single nucleotide polymorphisms [SNPs]) and 'G2' (an in-frame deletion of two amino acids) - confer resistance to Trypanosoma brucei but increase the risk of focal segmental glomerulosclerosis. More recently, fetal APOL1 variant alleles have been associated with preeclampsia. The overall level of circulating APOL1 is higher in women with preeclampsia than those without. Based on this, we hypothesized that trophoblast expression of APOL1 would be higher in placentas with maternal vascular malperfusion (MVM) than those without.

Methods: After obtaining IRB approval, our Laboratory information system was searched for placental cases meeting criteria for MVM (showing decidual arteriopathy of any kind, with or without infarcts or other features of MVM) along with gestational age-matched controls. 20 cases of MVM and 20 controls were selected. APOL1 expression was identified by immunohistochemistry (IHC) and evaluated in extravillous trophoblasts within the basal plate to generate an H-score (intensity of staining [0-3+] multiplied by percent of positive cells to generate a score of 0 to 300). Other cellular compartments of the placenta were also examined including amniocytes, fetal vessels, villous trophoblasts, decidua, fibrin, and maternal decidual vessels.

Results: All MVM cases and control placentas showed some degree of expression of APOL1 in various cellular compartments. APOL1 was expressed weakly in amniocytes and fetal vessels (endothelium and smooth muscle media cells). It was detected in villous trophoblasts (weak to moderate expression), maternal vessels, decidua, and fibrin. The extravillous trophoblasts showed a range of cytoplasmic APOL1 expression in MVM cases (range =10-150, mean=60) and controls (range=0-225, mean=83); the mean was not significantly different between the groups (Student's t-test p = 0.26).

Conclusion: APOL1 protein expression can be detected by IHC in the placenta. The protein is expressed in trophoblasts. We did not identify a difference in expression between MVM and non-MVM placentas, but larger studies (particularly those including known cases of fetal APOL1 variant alleles) may provide interesting biologic insights into the relationship between APOL1 and MVM and yield important diagnostic IHC tools for placental pathologists.

43

Congenital Cytomegalovirus Infection Is Associated with Congenital Rickets – A Retrospective Autopsy Study

E Chan, S Haider, W Yu, L de Koning; University of Calgary, Alberta Children's Hospital, Calgary, Alberta

Background: Congenital rickets due to maternal vitamin D deficiency is uncommon but well documented. Mahon et al. (2010), using 3D ultrasound, found that lower maternal serum 25-hydroxyvitamin D was associated with metaphyseal splaying (a radiologic finding seen in childhood rickets) of the fetal femurs, detected as early as 19 gestational weeks. In a separate study, Rieder et al. (2017) found that cytomegalovirus (CMV) infection led to a rapid, pronounced (by ~90%), and persistent decrease in expression of vitamin D receptor (VDR) mRNA in vitro. This was specific to CMV and not observed for other common human viruses (e.g. adenovirus, influenza). Recently, Robak et al. (2021) found that hematopoietic stem cell transplantation patients had lower VDR mRNA expression during CMV infection relative to pre-CMV infection. VDR encodes a nuclear receptor that plays a key role in regulating calcium and phosphate absorption and bone development. We therefore hypothesized congenital CMV (cCMV) infection could interrupt vitamin D metabolism and disrupt fetal/neonatal bone development.

Methods: This was a retrospective cohort study of autopsy reports from our pathology database, which included 15 years of data. We first identified all reports of fetal/neonatal demise in which cCMV infection was diagnosed (exposed group; n = 7). We matched them to 21 reports of demise due to either acute chorioamnionitis or acute placental abruption, without cCMV infection (3 per exposed report, randomly selected within the same gestational age). We additionally retrieved autopsy reports of congenital infections other than cCMV (2 herpes simplex, 3 parvovirus, 2 syphilis, 2 toxoplasma). The final sample size for the unexposed group (no cCMV infection) was 30. All observations in our study were independent of one another, as each autopsy report was associated with a different mother. Finally, a pediatric radiologist reviewed all radiographs, a perinatal pathologist reviewed histologic bone sections, and the findings were summarized.

Results: Radiographs were available for all autopsies. Metaphyseal splaying was observed in 4 of 7 reports (57%) in the exposed (cCMV infection)-group. No radiologic or histologic findings of congenital rickets were found in any of the reports from the unexposed (no cCMV infection)-group.

Conclusion: cCMV infection is strongly associated with congenital rickets. The pathogenesis is unclear, but likely involves the VDR, since VDR expression is downregulated during CMV replication in vitro and in vivo. Whether development of congenital rickets was due to the effect of CMV on the maternal, fetal, or placental VDR is unclear from our study, and will require further investigation.

44

Placental Features in Selective Reduction : A Retrospective Case Series

A Lafreniere[1], T Platero Portillo[2], D Kinnear[1], E Castro[1]; [1]Texas Children's Hospital, Baylor College of Medicine, Houston, Texas; [2]Baylor College of Medicine, Houston, Texas

Background: With improvements in assisted reproduction techniques (ART) and expansion of centers offering ART, there has been an increase in related complications. Multifetal pregnancies are a known complication of ART and are associated with maternal and perinatal morbidity and mortality, risks that increase with increasing fetal numbers. Radiofrequency, laser, and chemical techniques can be performed between 14- and 23-weeks gestational age (GA) for selective fetal reduction in multifetal pregnancies. These minimally invasive techniques have been shown to be safe and effective; however, the effects on the placenta have not been studied.

Methods: Records of the Pediatric Pathology Department were searched between January 1, 2011 and December 31, 2021 for cases of selective reduction in multifetal pregnancies. Ablation of vascular anastomoses in twin-to-twin transfusion resulting in demise were excluded. Pathology reports were reviewed to obtain demographic information, clinical history, and placental pathology. Statistical analyses were performed to assess for associations between findings.

Results: 1876 multifetal placentas were assessed during the study period, of which 8 met the inclusion criteria. Most cases selectively reduced 1 to 2 fetuses with one case reducing from 6 to 1. The mean GA at delivery was 35-5/7 weeks with a median GA of 36-2/7; there were no instances of demise post-reduction. While all cases delivered in the third trimester, only 37.5% of cases delivered at term. Placental weights ranged from: less than 3rd percentile (n=3); 25-50th percentile (n=2); 50-75th percentile (n=1); to 90-97th percentile (n=2). Pigment-laden macrophages were seen in half of all placental membranes and amnion/chorion nodosum was a common finding (37.5%). There were no cases of chorioamnionitis with only two cases showing acute choriodeciduitis/subchorionitis. Abnormal villous maturation was frequent (75%) and associated with preterm delivery (p=0.035); no association was observed between maturation and low placental weight (p=0.64). Basal plate inflammation and maternal vasculopathy cooccurred in two cases (p=0.005). Fetus papyraceus were identified in 75% of cases, at times embedded within the placenta.

Conclusion: Selective reduction reduces the maternal and perinatal risk of multifetal pregnancies. This series showed no post-reduction fetal demise with all deliveries occurring in the third trimester. Even in cases of preterm premature rupture of membranes, there were no incidents of chorioamnionitis, a frequent concern in prenatal intervention. Though significant pathology was not seen in this study, abnormal villous maturation was noted in association with preterm delivery. This study highlights not only the safety of selective reductions, but the overall limited effect on the placenta.

45

Placental Membrane Myofibers, Is It a Feature of Morbidly Adherent Placenta?

J Gulliver[1], M Bitar[2]; [1]Northwestern University Feinberg School of Medicine/Lurie Children's, Chicago, Illinois; [2]Northwestern University Feinberg School of Medicine, Chicago, Illinois

Background: Morbidly adherent placenta is thought to be related to the absence or deficiency of endometrium available for decidualization in an area of uterine scar. While basal plate myofibers (BPMF) might represent occult placenta accreta and convey a potential risk of morbidly adherent placenta, the significance of membrane myofibers (MMF) in the parietal decidua is poorly understood. MMF was first described in 2007. A study by Khong et al. suggested that MMF might represent the membrane counterpart of BPMF based on prototypical clinical and pathologic findings. To investigate if MMF is a feature of morbid adherence, we describe clinical and pathologic findings in placentas with incidental MMF.

Methods: This study is a survey of eight placentas submitted for pathologic review at our institution. Gross examination and standard histologic evaluation were performed on all placentas. Relevant obstetric clinicopathologic data were collected: patient age; gestational age; history of gravidity, history of Cesarean-section or uterine instrumentation; history of morbidly adherent placenta; indication for placenta examination; co-existing BPMF; and other placenta pathologic findings.

Results: Patients' age range was 29-36 (mean 33). 2/8 patients delivered prematurely in late third trimester, 4/8 patients had previous pregnancies and 2/6 had previous C-section or uterine instrumentation. None of the patients had history of morbidly adherent placenta or occult placenta accreta. Some indications for placenta examination included abruption (2/8), preeclampsia (1/8), and gestational diabetes (1/8). Each patient delivered an intact placenta. 2/8 placentas were small for gestational age. All placentas contained adherent MMF to the parietal decidua within the membrane rolls ranging from few to many myofibers forming nodular-like areas. 3/8 placentas additionally contained BPMF. Other pathologic features included acute chorioamnionitis with various maternal and fetal responses (5/8), chronic villitis (3/8), mural hypertrophy of membrane arterioles (2/8), intervillous thrombi (2/8), retroplacental/subchorionic hematoma with adjacent remote villous infarct (1/8), remote parietal decidua hemorrhage (1/8), and intramural fibrin deposition in a single fetal vessel (1/8).

Conclusion: None of the eight patients in this study had a known history of, or clinical suspicion for, morbidly adherent placenta. Co-exiting BPMF was present in 3/8 (37.5%) of placentas with MMF. Association of MMF with BPMF is documented in this study, however, the rate of association may be underestimated. A prospective study including a larger series of cases will be very helpful to assess if MMF is a reliable marker for morbidly adherent placenta in future pregnancies.

46

Improvements after Addition of Placenta Pathology Examination Order to Postpartum Order Set: an Institutional Experience

C Hughes, H Wang, H Correa, J Liang; Monroe Carell Children's Hospital at Vanderbilt University Medical Center, Nashville, Tennessee

Background: When our institution adopted a new electronic medical record (EMR) in November 2017, an order for placental pathology examination was built into the new EMR. However, the EMR order was rarely used. Instead, the traditional method of ordering placental pathology examination on a paper requisition was continued. In a time of great change, using a paper requisition was familiar to the labor and delivery staff, but had its drawbacks, including increased risk for error with handwritten submissions and incomplete requisition forms. Information such as the gestational age, the clinical indication and the mode of delivery was often missing from the hand-written requisitions. This information is essential to the pathologist reviewing the placenta and reporting clinically relevant findings.

Methods: The current placental pathology examination order was added to the pre-existing postpartum order set in our institution's EMR (Epic). An Epic Tipsheet was created and distributed to all labor and delivery faculty and staff to inform them of the change and how to use the order within the preexisting order set. The electronic order usage during the two-month period immediately following the "go live" date was monitored. Usage of electronic orders and numbers of incomplete requisitions in this period were compared to those during the 12-month period immediately prior to the go live date. A natural language search in CoPath was used to search for incomplete requisitions.

Results: The rate of electronic order usage has increased substantially from 5.1% to 73.4% after the addition of the placental pathology examination order to the postpartum order set ($p < 0.01$). The percentage of requisitions associated with incomplete clinical information was considerably lower in those that were ordered electronically through the order set compared to those that were ordered through paper requisitions (11.6% versus 18.8%, $p < 0.05$). Implementation of an electronic Tipsheet for clinical staff reduced the rate of incomplete requisitions ordered electronically from 12.0% to 9.4%. The overall rate of incomplete requisitions (paper and electronic) also decreased from 16.7% to 12.8% after the implemented changes.

Conclusion: Adding the placental pathology examination order to the preexisting postpartum order set, supplemented by a TipSheet, facilitated the use of the order by labor and delivery staff and decreased the rate of incomplete requisition forms.

47

Shallow Placental Implantation Recurs in Subsequent Pregnancies

S Ikegami[1], J Stanek[2]; [1]University of Cincinnati Medical Center, Cincinnati, Ohio; [2]Cincinnati Children's Hospital Medical Center, CIncinnati, Ohio

Background: Shallow placental implantation (SPI) has been recently reported as a distinct category of placental lesions, strongly associated with various types of adverse perinatal outcomes and other abnormal placental phenotypes. The objective of this study is to investigate the rate of recurrence of SPI lesions in subsequent pregnancies.

Methods: This preliminary retrospective study was performed on pairs of placentas from 24 women who delivered twice at the University of Cincinnati Medical Center. SPI diagnosis was made by showing one or more of the following histological lesions: increased amount of extra villous trophoblasts (>5 cell islands per section), >3 chorionic microcysts in the membranes or chorionic disc, and decidual clusters of >3 multinucleated trophoblasts. The frequencies of SPI lesions and the estimated recurrence rate were assessed. All statistics were computed using R and Excel.

Results: Of 48 placentas, 29 (60.4%) showed SPI lesion(s) and 19 (39.6%) did not. Among SPI placental pairs, in 10 women of 19 (52.6%) the SPI lesion(s) was present in both (Group 1), and in 9 women of 19 (47.4 %) in only one (Group 2). The average gestational age at delivery of the SPI placentas was shorter than the non-SPI placentas, 30.2 ±7.1 weeks vs 34.3 ± 5.4 weeks, respectively ($p< 0.029$); however, there was no statistically significant difference in the gestational age between Group 1 and Group 2. The frequencies of SPI lesions were: decidual multinucleate trophoblasts (55%), increased extra villous trophoblasts (40%), chorionic microcysts in the membranes (30%) and chorionic microcysts in the chorionic disc (15%) in Group 1, and 33%, 44%, 33% and 0% in Group 2, respectively. No statistically significant differences were found in the frequencies of each particular SPI lesion between Group 1 and Group 2 ($p>0.05$). However, the average number of positive SPI lesions was statistically higher in Group #1 (1.5 ± 0.6) than Group #2 (1.1 ± 0.3) ($p=0.036$).

Conclusion: Our results demonstrate a high recurrence rate of SPI lesions in subsequent pregnancies, comparable to other recurrent placental lesions such as acute chorioamnionitis, massive perivillous fibrin deposition or chronic villitis of unknown etiology. Therefore, the histological recognition of SPI in the placenta may be important for management of future pregnancies because of the increased risk of associated complications.

48

Pulmonary Miliary Mycobacterium Tuberculosis in a Neonate: A Case Report and Review of Institutional Guidelines for Infection Control

E Schuele[1], Y Estrella[2], K Patel[2]; [1]Baylor College of Medicine, Houston, Texas; [2]Texas Childrens Hospital, Houston, Texas

Background: M. tuberculosis infection is rare in the United States; rarer still in neonates. We present a case of fatal miliary tuberculosis in a 36 day old, preterm, female, twin neonate (born 30 6/7 weeks gestation).

Methods: Restricted (chest and abdomen) autopsy was performed after informed consent. IRB approval is in place to present this case. Routine and ancillary testing was done to establish the diagnosis.

Results: A 33 day old female infant born to a 38 year old G3P1 mother at 30 6/7 weeks of a twin (dichorionic and diamniotic) gestation (corrected age: 35 3/7 days) with Apgar 8 and 9 at 1 and 5 minutes. While being hospitalized, she developed fever and respiratory distress with bilateral infiltrates on chest X-ray at 3 weeks of age. Multiple blood cultures were negative. Despite aggressive management, she continued to deteriorate, required intubation within a week, and passed away in two weeks. Autopsy showed a well-developed female infant, appropriate for age, without any congenital anomalies. Bilateral lungs and hilar lymph nodes showed diffuse necrotizing granulomatous inflammation with abundant acid fast bacilli. Mycobacterium tuberculosis (MTb) was confirmed by PCR test. Background lungs showed acute diffuse alveolar damage. MTb was not seen in any other organs, including the placenta. Clinical team was contacted with the results. Mother had traveled from Nigeria one week before the delivery. Both mother and twin were asymptomatic; only the twin was positive by tuberculin test and received appropriate prophylaxis. Other neonates from the nursery and the medical care team were tested and monitored for symptoms. No other active infections were detected. Father had briefly been in contact with the deceased twin and could not be contacted.

Conclusion: In non-endemic regions, neonatal tuberculosis is rare, but documented within NICUs. A high index of suspicion is required to diagnose tuberculosis infection in the neonatal population, as infants are more likely to have negative culture and tuberculin skin test (TST) results, equivocal chest X-ray findings, and atypical symptoms of disease. While vertical transmission can occur, nosocomial and/or community transmission are important considerations along with the infection mitigation efforts of the institution.

49

Indeterminate Cell Histiocytosis: Postmortem Diagnosis of a Rare Disease in an Infant.

A Lafreniere, D Kinnear, M Elghetany, K Patel; Baylor College of Medicine, Texas Children's Hospital, Houston, Texas

Background: Indeterminate cell histiocytosis (ICH), or indeterminate dendritic cell tumor, is a rare neoplasm of 'indeterminate cell' origin, hypothesized to be a precursor to Langerhans cells. ICH presents most frequently in the skin, followed by lymph nodes, spleen, and rarely systemic. It occurs primarily in adults. We report autopsy findings of disseminated ICH diagnosed in the postmortem setting in a 6-week-old infant.

Methods: Unrestricted autopsy was performed after an informed consent. IRB approval is in place for reporting this case. All routine and ancillary testing performed for establishing the diagnosis.

Results: An otherwise healthy, term, female neonate was admitted at 2 weeks age with an Escherichia coli urinary tract infection for 4 days. She was persistently thrombocytopenic during admission (platelets 29 K/uL at discharge). Platelets recovered to 92 K/uL at 2 weeks of outpatient follow up. At 6 weeks age, she re-presented with fever, pancytopenia, elevated inflammatory markers (ferritin >3,000 microg/L, lactate >20mmol/L), and ultrasound showing hepatosplenomegaly with diffuse innumerable echogenic foci in both organs. SARS-CoV2 PCR and preliminary microbiology cultures were negative; ANC was 5.83x103 microL. An echocardiogram showed appropriate biventricular function. She was transferred to our hospital for rapid onset respiratory distress and progressive multisystem organ failure; however, she decompensated and died on arrival. Autopsy showed diffuse histiocytic proliferation involving the lymph nodes, bone marrow, liver, and spleen with focal involvement of bilateral lungs that were diffusely hemorrhagic. Neoplastic cells resembled Langerhans cells with abundant pale cytoplasm and oblong vesicular nuclei with occasional clefting. They were immunoreactive for S100 and CD1a; and negative for CD207, CD163, CD68, fascin, and factor XIIIa. Eosinophils were not increased. No Birbeck bodies were seen by ultrastructural exam. BRAF V600E was not detected by RT-PCR. Coagulase-negative Staphylococcus was detected in postmortem blood culture.

Conclusion: ICH is a rare disease described in the WHO Classification of Tumours of Haematopoietic and Lymphoid Tissue (Revised 4th Edition), with a single report of neonatal death in 1999. Like other histiocytic/dendritic cell tumors, ICH can occur in association with hematologic neoplasms; however, no concurrent lymphoma/leukemia was identified. Varying clinical outcomes have been reported, ranging from spontaneous regression to rapid progression, the latter reflecting the clinical course observed. Review of the literature suggests that rapid progression and complications of infection, as seen in this case, are more common in the pediatric setting, warranting increased vigilance by pathologists and clinicians for this serious but rare entity.

2021 Resident Recruitment Award Recipients

1

Infantile Diarrhea Secondary to an Acquired Duodeno-Colonic Fistula: Informed by Upper GI Biopsies

Y Zhou; University of Minnesota, Minneapolis, Minnesota

Background: Diarrhea in young infants encompasses a wide range of etiologies that include infectious disease, dietary-triggers, prematurity, anatomic defects, and congenital abnormalities[1]. Among these, the clinical symptoms often overlap, rendering the diagnosis challenging and requiring consideration of the clinical presentation, imaging, laboratory tests, and gastrointestinal endoscopy and biopsy findings. Duodeno-colonic fistula is a rare disorder reported as a complication of malignancy, duodenal ulcer, inflammatory bowel disease, and duodenal diverticulum[2]. It is extremely rare in young infants and children. Here we report a case of infantile diarrhea secondary to an acquired duodeno-colonic fistula, in which the histologic examination of gastrointestinal (GI) biopsies was instrumental in determining the cause of diarrhea.

Case presentation: A 34 day-old female infant, born at term, presented to the emergency department with a 3 day history of irritability, diarrhea (more than 20 watery yellow stools per day), and weight loss. She had been discharged 3 days earlier from a hospitalization that included repair of a duodenal atresia by a duodeno-duodenostomy on day of life (DOL) 3. There was an *E. coli* and *Enterococcus faecalis* bacteremia from post-operative day (POD) 3-7. Enteral feeds began on POD 8 with parenteral nutrition continued until she was gradually transitioned to complete enteral feeds and discharged on POD 28. An upper GI study on POD 4 showed anastomotic narrowing that improved on a POD 17 study. Both studies showed an intact anastomosis with no leaks.

On current presentation, her vital signs were stable, her physical exam was unremarkable, and her laboratory studies showed a non-anion gap metabolic acidosis and hypernatremia. She was admitted for IV hydration, electrolyte correction and treatment of an ileus possibly secondary to electrolyte abnormalities. Abdominal imaging showed nonobstructive bowel gas distention with no pneumatosis. An extensive workup included an enteric pathogen panel (PCR) and tests for C. diff. toxin B (PCR), stool ova and parasites, stool reducing substances, and alpha 1-antitrypsin. All were negative. Stool elastase was low. Small bowel follow-through showed no evidence of intestinal obstruction. Her diarrhea improved with initial management; however, several attempts to increase enteral feeding resulted in worsening of the diarrhea. Her hospital course was further complicated by a new fever, *E. coli* and *Lactobacillus* bacteremia and *Candida* fungemia since DOL 47. Because her diarrhea was severe and did not resolve, upper GI endoscopy and sigmoidoscopy with biopsies were done, and congenital diarrheal disorders were considered.

Endoscopic findings included a nonbleeding ulcer in the pre-anastomotic duodenum, a grossly normal proximal duodenum, and difficulty reaching the distal duodenum. Biopsies of the pre and post-anastomotic duodenum and sigmoid colon were taken for routine processing, and additional duodenal biopsies were fixed in glutaraldehyde for possible ultrastructural study.

Biopsies from the pre-anastomotic duodenum and sigmoid colon showed no histologic abnormalities. The histology of the post-anastomotic duodenum showed no villous architecture and oddly appeared to resemble colon. Due to the highly unlikely possibility that colonic mucosa would be found in the duodenum, additional evidence was felt needed to remove any doubt. Immunophenotypic markers were applied to make the distinction, using the pre-anastomotic duodenum and sigmoid colon as controls (Figure 1). The pre-anastomotic duodenum showed no staining of enterocyte nuclei with SATB2, strong CD10 positivity of the brush border, and absence of brush border staining with CEA. In contrast, both post-anastomotic duodenum and colon showed a similar profile with positive staining of

enterocyte nuclei with SATB2, spotty positivity of the brush border with CD10, and strong staining of the brush border with CEA. These findings confirmed that the post-anastomotic duodenal biopsies were colonic mucosa indicating that the biopsies were either the product of colonic metaplasia or actually from the colon. The latter could only be possible if there was a duodeno-colonic anastomosis or fistula. Microvillus inclusion disease, tufting enteropathy, and enteroendocrine cell dysgenesis were excluded by CD10, MOC31, and chromogranin immunostains, respectively[3].

Based on the above histologic findings, an upper gastrointestinal series with small bowel follow-through was performed, showing opacification of colon at the level of hepatic flexure during early gastric emptying (Figure 2), supporting the presence of an acquired duodeno-colonic fistula. It was felt that there was an anastomotic leak at the site of the original duodeno-duodenostomy which led to a duodeno-colonic fistula. A fistula to the transverse colon near the hepatic flexure was identified and repaired during the subsequent surgical procedure. The patient's diarrhea resolved, and she was eventually able to tolerate oral feedings upon discharge. 12 months after the surgical repair, there was no recurrence, and the patient experienced appropriate weight gain and met all developmental milestones.

Discussion: An extensive workup did not identify the cause of the diarrhea in this case due to nonspecific symptoms and the extremely unusual etiology in this young infant. Duodeno-colonic fistula presenting as diarrhea has only been rarely reported in children[4], and in an odd twist, one case secondary to ingestion of a construction nail by a 3 year-old was asymptomatic 30 days from ingestion[5]. In the current case, the most likely cause for the fistula is a postsurgical anastomotic leak leading to development of a fistula. Given the architectural distortion seen in small intestine in some diarrheal disorders, loss of villous architecture may lead to a consideration of a host of disorders prior to the consideration that one is viewing colon in a duodenal biopsy. Hence, the judicious application of a combination of immunohistochemical markers including SATB2, CEA and CD10 to distinguish between the phenotypes of small and large intestine6, [7] can be an effective tool in such situations. In conclusion, this case highlights the indispensable value of careful histologic examination of GI biopsies in the multidisciplinary care of young infants with intractable diarrhea.

Pre-anastomotic Duodenum Post-anastomotic Duodenum Sigmoid Colon

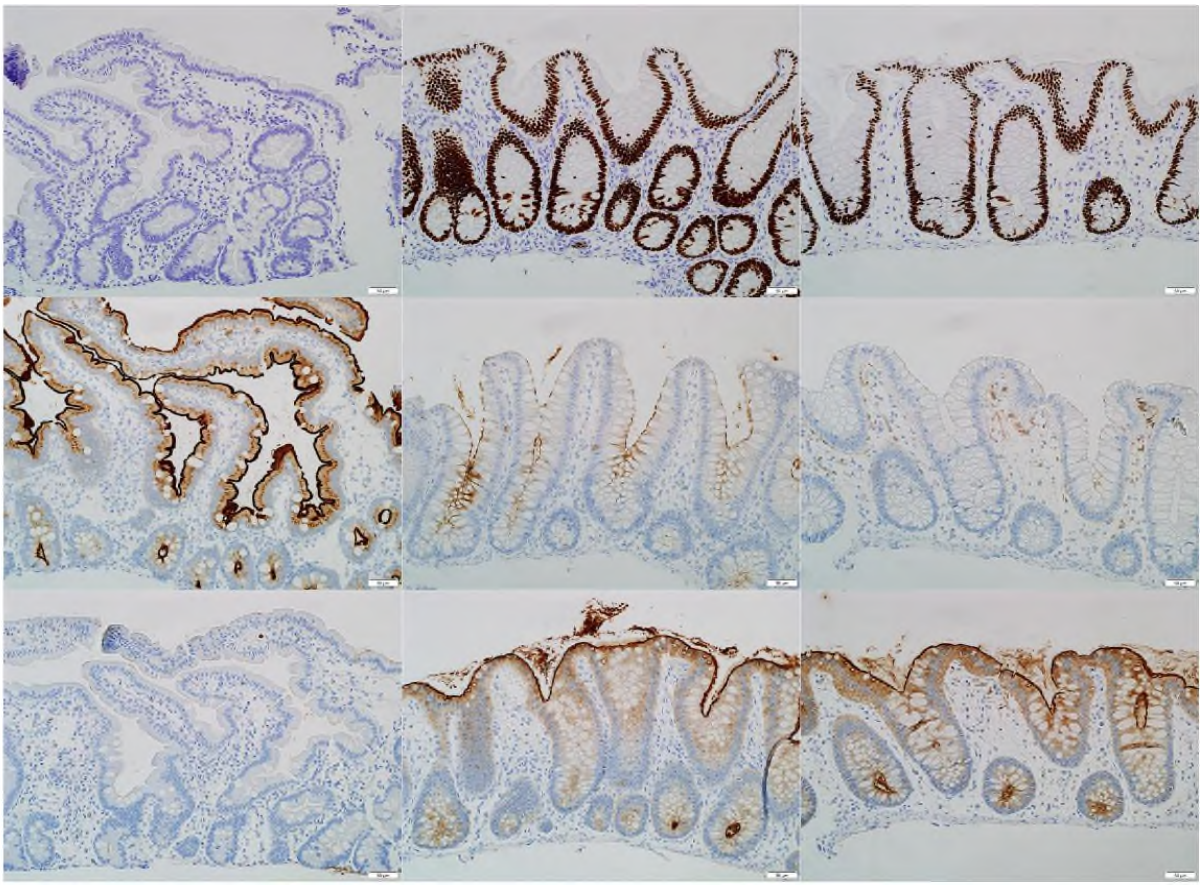

Figure 1: The above immunohistochemical profile shows that the post-anastomotic bowel has a phenotype consistent with colon (all photos captured with a 20x objective).

Figure 2: Select last image hold from an upper gastrointestinal series; the patient in the left anterior oblique position. On earlier images (not included) there was concern for abnormal communication between the repaired duodenum and colon (in the region of the arrow). This 5 minute delayed image demonstrates the black intraluminal contrast filling the colon prematurely (arrowhead), confirming the suspicion of duodeno-colonic fistula.

2

Novel *FOXP3* Mutation Associated with Refractory Diarrhea, Late-Onset Necrotizing Enterocolitis, and An Aggressive Course

S Schauwecker; Vanderbilt University, Nashville, Tennessee

Background: Pediatric congenital enteropathies are a rare and heterogeneous group of disorders characterized by severe diarrhea and intestinal failure. The syndrome of immune dysregulation, polyendocrinopathy, enteropathy, X-linked (IPEX syndrome) is an important cause of autoimmune enteropathy. IPEX is caused by loss-of-function mutations in the gene encoding the forkhead box P3 (FOXP3) transcription factor, located on the X chromosome. FOXP3 is critical for proper development of regulatory T cells, which are correspondingly decreased in patients with IPEX. Without proper regulatory T cells, there is impaired suppression of inflammatory responses, leading to multisystem autoimmune manifestations. Most patients with IPEX syndrome develop early-onset enteropathy with watery diarrhea, skin manifestations including eczema and exfoliative dermatitis, and autoimmune endocrinopathies including type 1 diabetes and thyroid disease (1-3). Other common manifestations include cytopenias and renal disease (1-3). While most cases are diagnosed before 1 year of age, IPEX can also present prenatally or in older children (1, 4).

Because infantile diarrhea has a broad differential diagnosis, precise classification is critical to guide proper treatment. Patients with IPEX are treated with immunosuppression and/or hematopoietic stem cell transplant. However, IPEX is typically fatal without proper treatment, highlighting the need for prompt diagnosis. Gastrointestinal biopsies show variable findings but are generally characterized by small intestinal villous atrophy, a mixed inflammatory infiltrate of the lamina propria, cryptitis and crypt microabscesses, and increased crypt apoptosis (1, 2, 5, 6). Goblet cells and Paneth cells are often decreased (2, 5, 6). Because IPEX can present with a broad spectrum of both clinical and histopathologic findings, increased awareness of this spectrum is critical for a prompt and accurate diagnosis. Here, we report a case of a term infant with IPEX syndrome presenting with chronic diarrhea and necrotizing enterocolitis, illustrating a particularly severe gastrointestinal manifestation of this syndrome.

Case Description: A 2 month-old, previously full term, male infant presented with weight loss and failure to thrive in the setting of chronic watery diarrhea and 2 weeks of vomiting. He had a history of congenital hypothyroidism, identified on newborn screening. At the time of presentation, he weighed 1 lb below his birthweight. Abdominal ultrasound and upper gastrointestinal tract fluoroscopy showed no evidence of pyloric stenosis, obstruction, or malrotation. Infectious stool studies were normal. The clinical differential was broad and included cow milk protein allergy, protein induced enterocolitis, infectious etiologies, and congenital enteropathies. He was admitted to the hospital and started on nasogastric tube feeds, but developed worsening diarrhea, lethargy and hypotension. He required fluid resuscitation and eventual intubation. Abdominal X-ray and ultrasound showed diffuse portal venous gas and pneumatosis intestinalis. Soon after, his abdomen became distended, and his hypotension worsened. He was taken for an exploratory laparotomy, which intraoperatively showed an area of ileal necrosis with adjacent areas of patchy ischemia. A 16 cm portion of ileum was resected. Pathology revealed patchy full thickness ischemic necrosis, focal mucosal ulceration, frequent crypt epithelial apoptosis, and mucosal and serosal acute inflammation (Figure 1A-1B). Congenital enteropathies were thought to be less likely given these findings, and the patient completed a course of antibiotics for necrotizing enterocolitis.

Despite initial clinical improvement, the patient had continued diarrhea, emesis with enteral feeds, and severe hypotension. His course was further complicated by cytopenias, hypoalbuminemia, hypogammaglobulinemia, and proteinuria. Given the continued diarrhea despite resection and antibiotic treatment for necrotizing enterocolitis, clinical suspicion for a congenital enteropathy –

including IPEX – was growing. Biopsies of the duodenum, stomach, ileum and sigmoid colon showed complete loss of surface epithelium and near-complete loss of crypts (Figure 1C, ileum), with residual pits present only in the stomach. The prior ileal resection material was reviewed for comparison and showed a reduction of goblet cells and Paneth cells, in addition to the increased crypt epithelial apoptosis (Figure 1B). These findings raised the consideration of an autoimmune disorder such as IPEX. Concurrently, next generation sequencing revealed a novel pathogenic variant in *FOXP3*, c.1010G>C (p. Arg337Pro), establishing the diagnosis of IPEX syndrome. The patient was started on immune suppression and is currently being evaluated for eventual stem cell transplant.

Figures

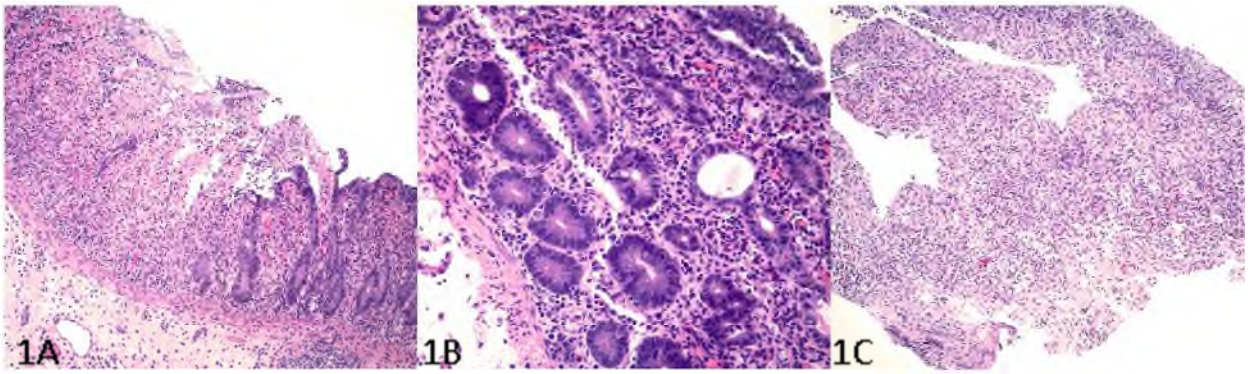

Summary: This case illustrates a highly unusual presentation of IPEX syndrome with particularly severe clinical and pathologic findings. To our knowledge, this is the first reported case of IPEX syndrome presenting with necrotizing enterocolitis. The severity of the histopathologic findings, with ischemic necrosis progressing to near-total loss of epithelial cells in multiple gastrointestinal sites, is beyond that previously described in IPEX. In addition, the pathogenic *FOXP3* variant identified (c.1010G>C, p. Arg337Pro) has not been previously reported. Whether this novel missense mutation causes this unique phenotype remains to be determined. This mutation results in substitution of arginine for proline in a residue of the forkhead domain, which is critical for DNA binding. Previous studies of genotype-phenotype correlations of *FOXP3* mutations in IPEX have shown mixed results (1-3, 7). One study has shown forkhead domain mutations to be associated with autoimmune hemolytic anemia, while an increased risk of death was found with mutations in the repressor domain, intron 7, or poly A sequence (3). While more work is needed, this promises to be an exciting direction in better understanding IPEX pathophysiology. With the growing availability of next generation sequencing, the diagnosis of IPEX is being made more frequently, suggesting that the true incidence may be underestimated (7). In particular, this has led to increasing awareness of IPEX in milder cases of enteropathy and in older patients than were traditionally associated with IPEX syndrome (7). However, this case illustrates the potential severity of both the clinical and histopathological findings in IPEX, increasing our awareness of the other end of the spectrum of IPEX presentations. This case highlights the importance of maintaining a broad differential within this unique and challenging area of pediatric pathology.

"Unboxing" the pulmonary effects of *TBX4* germline mutation, an autopsy case study Introduction

E Doughty; University of Colorado Anschutz, Aurora, Colorado

Molecular medicine advances have identified multiple genetic and genomic drivers of pulmonary arterial hypertension (PAH). In this autopsy case, we explore the long-term clinical implications and histopathologic alterations of childhood-onset PAH in the setting *TBX4* heterozygous germline mutations.

Clinical history: A 12-year-old male presented for surgical correction of bilateral genu valgum and was observed postoperatively to have persistent nocturnal oxygen desaturations. Further investigation revealed non-reactive systemic PAH. Over the next five years, he demonstrated a continuous decline in exercise tolerance and right ventricular function despite maximized pulmonary hypertensive therapy. As an additional downstream effect of the progressive and treatment-refractory PAH, he developed portal hypertension complicated by esophageal varices and gastropathy resulting in multiple episodes of hematemesis. At 19 years of age, following a failed geographic relocation to sea level, a slowly enlarging pericardial effusion was discovered on imaging. During the last five years of life he experienced worsening biventricular congestive heart failure and was hospitalized on multiple occasions for pneumonia and increasing oxygen requirements. The patient and his family opted out of lung transplantation and at 24 years of age he was transitioned to palliative-focused care. He died four weeks later while hospitalized for worsening hypoxic respiratory failure and anasarca. Permission for a lung-restricted autopsy was granted. In addition to PAH, the patient's clinical history is significant for autism spectrum disorder, keratoconus, angiofibromas, infantile renal tubal acidosis, and growth restriction. Karyotype analysis revealed a de novo chromosome 3 deficiency (46, XY, del(3)(q26.2q26.32)) of unknown significance. Germline genetic testing performed in his late teenage years revealed a heterozygous missense variant in the *TBX4* gene (p.G106C).

Postmortem findings: Autopsy findings demonstrated numerous changes associated with PAH and *TBX4* mutation: dense, heavy lungs with incomplete horizontal fissure of right lung (Figure 1), cyanosis of the lips and fingers, an enlarged thoracic cavity, and valgus rotation of the lower extremity joints. Evidence of downstream sequelae included cardiomegaly with massive hemopericardium significantly reducing the left pleural space, marked lower extremity edema, pleural effusions, and superficial skin breakdown along the spine from prolonged bed rest.

Figure 1: *Left* - Incomplete horizontal fissure of the right lung; *Middle* - Dense heterogeneous parenchyma and infarct cavities; *Right* - Intravascular dye injection highlighting atypical pleural vascular patterns

Maldevelopment of all lung compartments was evident histologically: simplified, enlarged airspaces with back-to-back bronchiolar profiles, mesenchymal elements, pleural and lymphatic vessel muscularization, plexiform lesions, and recruited intrapulmonary bronchopulmonary vascular anastomoses (IBA) (Figure 2). Additional findings of long-standing vascular remodeling included smooth muscle hypertrophy and vessel wall hyalinization, obliteration of vascular lumens, and recanalization allowing for recruitment of IBA. The endothelium, which is susceptible to shear force injury, likely experienced increased blood flow through these transformed pathways as lung injury progressed, possibly causing thromboses and subsequent parenchymal infarcts.

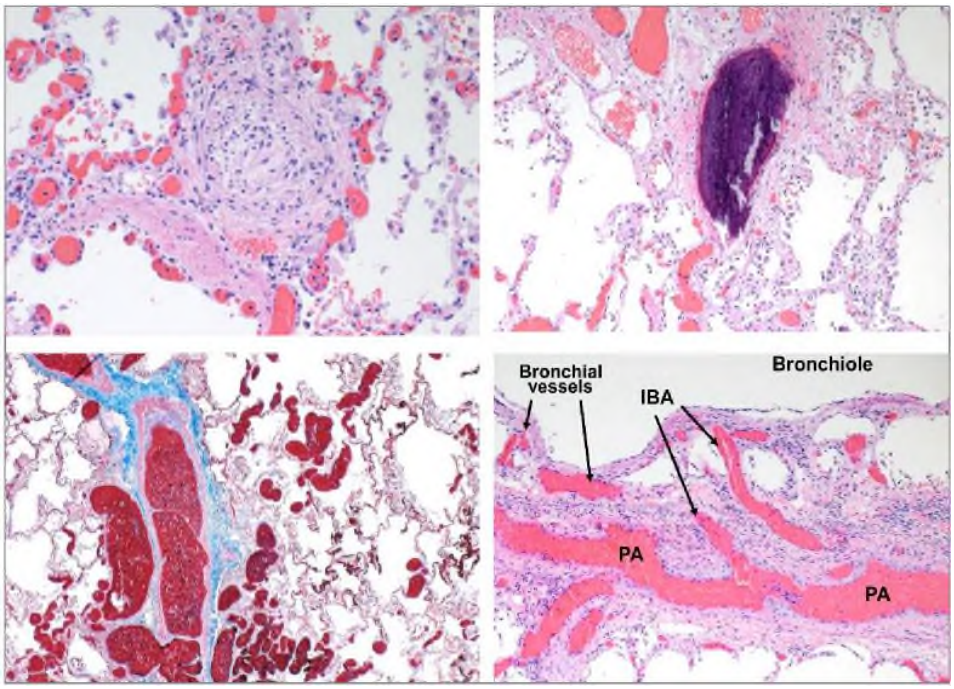

Figure 2:

Upper left - Pulmonary artery lumen obliteration and wall muscularization (H&E, 200x)

Upper right - Ectopic bone formation and stromal vessel dilatation with congestion (H&E, 100x)

Lower left – Plexiform lesion of a pulmonary artery, note the glomus-like capillary proliferation (Trichrome, 40x)

Lower right –Intrapulmonary bronchopulmonary anastomoses (IBA) allow blood flow between bronchial vessels and pulmonary artery (PA) branches creating right to

Discussion: Prolonged pulmonary hypertension, defined as increased pulmonary vascular resistance exerted on the blood entering the lungs for gas exchange, can result in a sequence of long-term sequelae starting with right heart failure and including portal hypertension, edema, and renal failure. Patients presenting in infancy are at a markedly increased risk of persistent patent ductus arteriosus or atrial septal defect due to the increased right-sided heart pressures but are also at an increased risk of additional congenital heart defects. An association between pediatric onset of PAH and genetic variations coding for the T-box transcription factor 4 (Tbx4) protein are increasingly recognized. The *TBX4* gene, located at chromosome 17q23, codes for the Tbx4 protein expressed in developing lung tissue and contributes to airway branching. Additionally, Tbx4 is involved with hind-limb formation. One study demonstrated a >75% overlap of patients with *TBX4*-associated PAH and skeletal anomalies[2]. Syndromic presentation of *TBX4* variation is known as small patella syndrome or ischiocoxopodopatellar syndrome and includes hypoplasia of the patella and anomalies of the pelvis and feet, as seen in this case. Neurodevelopmental disorders are highly prevalent in this patient group. Detrimental variations include deletions of the entire locus and neighboring genes as well as point mutations. In the current case, the *TBX4* mutation, present on only one of two genes, is a single missense substitution resulting in a coding variation of one amino acid. Observations of patients with a wide range of *TBX4*-variant presentations suggests that the amount of normal/abnormal protein expression does not correlate with clinical symptomatology. Histopathologic findings of lung tissue show abnormalities in not only the vascular structures, but also the airways, alveoli, and interstitium. Over time and under the influence of abnormal Tbx4 protein, pulmonary tissue remodels resulting in worsening PAH; by young adulthood, end-stage lung disease requires transplantation. Importantly, marked *TBX4*-related lung maldevelopment has been linked to lethal neonatal PAH cases.

Conclusion: This is a unique case of a 24-year-old who died due to complications of a germline *TBX4* variant. Due to the autopsy restriction to the lungs only, extent of cardiac remodeling and the origin of massive hemopericardium could not be assessed but likely played a role in the patient's demise. The maldeveloped background lung, in the setting of vascular restriction from thromboses and PAH, demonstrated innumerable infarcts which additionally impaired gas exchange. The oxygen demand of the lungs likely exacerbated the patient's known congestive heart failure and hemopericardium, which ultimately led to demise. Based on autopsy findings and clinical pathologic correlation, this patient's immediate cause of death was judged to be hypoxic respiratory failure, while the underlying cause of death was attributed to *TBX4* variant-associated PAH.